Applied Spatial Analysis and Policy (2026) 19:39
https://doi.org/10.1007/s12061-025-09789-6

Enhancing Deep Learning-based Crime Hotspot Predictions With Theory-based Environmental Risk Scores

Tugrul Cabir Hakyemez[1] · **Bertan Badur**[1,2]

Received: 2 January 2025 / Accepted: 20 December 2025
© The Author(s) 2026

Abstract

This study introduces a novel network-based crime risk score, the Street Segment Risk Score (SSRS), designed to enhance crime hotspot predictions on street networks. The SSRS evaluates the risk of individual street segments by incorporating the dynamic spatial influence of nearby urban features on local crime patterns. Our dataset comprises all reported incidents of robbery (n=2,016) and theft (n=31,493) from 2015 to 2018 in Chicago's Central Side (CS). We developed both daily and intraday crime hotspot prediction models that integrate the SSRS and compared their performance—with and without the SSRS—using two graph-based deep learning algorithms, Graph WaveNet (GWNet) and the Spatiotemporal Graph Convolutional Neural Network (STGCN); a traditional deep learning model, Long Short-Term Memory (LSTM); and two baseline methods, Multilayer Perceptron (MLP) and Spatiotemporal Network Kernel Density Estimation (STNetKDE). Results indicate that incorporating the SSRS improves daily robbery hotspot prediction accuracy by up to 5.3% and intraday theft prediction accuracy by as much as 33%. The proposed SSRS demonstrates strong potential to support more precise, street-level security interventions by enhancing daily and intraday crime hotspot predictions.

Keywords Crime hotspot prediction · Deep learning · Environmental crime risk · Spatiotemporal graph learning

✉ Tugrul Cabir Hakyemez
tugrul.hakyemez@bilgi.edu.tr

✉ Bertan Badur
badur@bogazici.edu.tr

[1] Department of Management Information Systems, Istanbul Bilgi University, İstanbul, Turkey

[2] Department of Management Information Systems, Bogazici University, Istanbul, Turkey

Published online: 14 February 2026

Introduction

The ability to predict when and where crime will occur has long been of interest in urban research due to its significant potential to enhance public safety and optimize resources (Wang, 2017; Smith, 2018). For this purpose, past researchers have often used prospective methods that predict the next crime locations based on existing ones (Bowers et al., 2004; Mohler et al., 2011; Rosser et al., 2017; Zhang & Cheng, 2020). As a popular prospective method, Predictive Crime Hotspot Mapping (PCHM) aims to predict areas with heightened crime risks on a map for upcoming time periods. A key element in PCHM is a risk surface, which represents geographical units within an area of interest along with their associated crime risk densities on a map. These densities are operationalized through a spatiotemporal kernel function, which calculates the risk density for each unit based on its crime history and that of its neighboring units. Theoretically, this approach is grounded in the boost hypothesis, which suggests that a crime event temporarily elevates the risk of further crimes in its vicinity (Bowers et al., 2004; Rosser et al., 2017; Zhang & Cheng, 2020; Johnson & Bowers, 2004). This transient risk often stems from active offenders revisiting locations where they have succeeded previously, driven by the familiarity of the area and the expectation of further rewards with minimal risk and effort. This behavior is grounded in Rational Choice Theory (RCT)(Cornish & Clarke, 1987), which portrays offenders as purposive agents who choose between legal and illegal actions based on rational cost-benefit analyses. Optimal Foraging Theory (OFT) (Johnson & Bowers, 2004) situates these rational calculations within an environmental context that weighs potential benefits (rewards) against the costs associated with committing the offence (Vandeviver et al., 2023). Offenders are likely to revisit past crime scenes because developed spatial familiarity not only reduces the effort required to navigate the environment but also minimizes risks by facilitating the identification of potential threats.

However, there may be cases where unaffiliated offenders (i.e., foragers) choose to commit crimes in familiar places regardless of their previous exposure to these locations. The flag (i.e., risk heterogeneity) hypothesis addresses these instances by focusing on the vulnerability of targets across urban environments (Johnson & Bowers, 2004). Accordingly, beyond the criminal history emphasized by the boost hypothesis, specific environmental characteristics may make targets more attractive to offenders. Overcrowded subway stations (Irvin-Erickson & La Vigne, 2015) or isolated streets near pubs and liquor stores (Ratcliffe, 2012) are examples of locations that offer rewards to "foragers" with low risks and minimal cost (Johnson et al., 2009). A viable approach to contextualizing these environmental vulnerabilities (i.e., the flags) involves incorporating theory-based crime risk indicators (Groff & La Vigne, 2002) that can capture environmental risk level changes. Hence, integrating the environmental context into crime risk predictions represents a significant research avenue that could enhance PCHM methods.

Past research often associates changing target vulnerabilities with the crime opportunities they offer to offenders (Brantingham & Brantingham, 1981; 1995). From the perspective of Routine Activity Theory (RAT), this opportunity arises when a suitable target encounters a motivated offender in the absence of a capable guardian (Cohen & Felson, 1979). Crime Pattern Theory (CPT) suggests that these opportuni-

ties are concentrated around particular urban features that attract large crowds or possess characteristics conducive to crime (Brantingham & Brantingham, 1981; 1995). The extent to which an urban feature facilitates these opportunities can be seen as a "flag", signaling fertile ground for offenders (Caplan et al., 2011). The opportunity field around these features determines their "spatial influence" on crime (Ratcliffe, 2012), often operationalized by a decaying cumulative crime density based on distance from the origin point (Ratcliffe, 2012; Wheeler, 2019; Hakyemez & Badur, 2021). The density peaks at the location due to the local effect and decreases through its immediate vicinity (i.e., spatial diffusion effect) (Wheeler, 2019).

A key driver of the hypothesized spatial influence is human activity around urban features, which amplifies the effect and extent of this influence (Groff, 2017). This ambient human activity is not constant but shows temporal variations throughout the day or week (Habermann & Ratcliffe, 2015). A time-geography perspective (Pred, 1981; Ratcliffe, 2006). accounts for these variations by examining generic group movement patterns and human activity at specific locations over time. For example, on a typical workday, individuals follow a route from home to the office, which may include public transit and occasional stops at grocery stores, with location changes reflecting the time of day. Similarly, weekly fluctuations occur, with the city's activity center shifting from business to entertainment districts during weekends as people socialize (Habermann & Ratcliffe, 2015; Bernasco et al., 2017). An environmental risk surface capturing this dynamic spatial influence could enhance Predictive Crime Hotspot Mapping (PCHM) methods by facilitating more accurate crime risk calculations for geographical units across an area.

A significant breakthrough in machine learning was achieved in the past decade with the introduction of Deep Learning (DL) (Krizhevsky et al., 2012; Goodfellow et al., 2016). Like many other fields, these advanced technologies have benefited crime prediction techniques, demonstrating improved predictive accuracies compared to the traditional counterparts (e.g., Random Forest, ARIMA, KDE)(Huang et al., 2018; Zhuang et al., 2017; Safat et al., 2021; Gu et al., 2024). In DL-based techniques, researchers often divide a region into a series of arbitrarily sized grids and generate predictions for each grid in the next time step. However, this approach has several problems. First, the arbitrarily shaped units are prone to the Modifiable Areal Unit Problem (MAUP) (Cheng & Adepeju, 2014), leading to unstable predictive performances based on the selected grid size. Second, since human activity is mainly constrained to street networks, risk predictions for areas beyond human activity (e.g., lakes and seas) remain unrealistic. Third, the approach distorts the crime risk distribution using artificial prediction units, negatively impacting predictions. Lastly, because patrol routes are also limited to street networks, the grids may not offer feasible routes for police patrolling (Rosser et al., 2017). Past research has well documented the superiority of graph-based algorithms over traditional deep learning (DL) approaches, such as LSTM and Recurrent Neural Networks (Hakyemez & Badur, 2023; Gu et al., 2024), primarily due to their ability to capture network topology and spatiotemporal dependencies between crime incidents. In summary, any DL-based PCHM implementation should operate within a network-constrained space to produce predictions that more effectively identify locations for targeted security interventions.

The current study introduces a novel network-based risk score called the Street Segment Risk Score (SSRS). This score represents the first attempt to quantify the dynamic crime risk (i.e., intraday and weekly) of street segments based on the spatial influences of urban features they host. Unlike methods that count the number of urban features of selected types in street segments (Hipp et al., 2021) or aggregate static crime risk scores calculated for urban features at non-network units like neighborhoods (Drawve et al., 2016), the SSRS offers a unique network-based approach. The model dynamically evaluates street segment crime risks, adapting to the evolving spatial influences and interactions of urban features. This interaction is quantified by incorporating a novel risk score, the Local Risk Score (LRS), which aggregates crime densities at locations of urban features using various Distance-aware Risk Signal Functions (DRSF) (Hakyemez & Badur, 2021). These functions model the dynamic spatial influences of urban features on crime throughout the day and week within a specified network bandwidth. Representing street segments with their SSRSs allows for creating a theory-based auxiliary risk surface, enhancing prospective PCHM. Despite recent attempts to integrate auxiliary risk surfaces, such as those incorporating co-occurring park events (Hakyemez & Badur, 2023), into DL-based PCHMs on street networks, our study stands out by devising a unique, theory-based crime risk score for street segments.

The methodology begins with calculating SSRS values based on five key urban features (i.e., bus stops, fast-food restaurants, gas stations, grocery stores, and pubs) and two crime types (i.e., robbery and theft) across two temporal models: intraday (First Shift: 00:00–07:59, Second Shift: 08:00–15:59, Third Shift: 16:00–23:59) and weekly (weekday-weekend). We then test whether including SSRS values improves the predictive performance of the selected algorithms. To evaluate effectiveness, we created another auxiliary static risk surface that simply counts the selected urban features in street segments. Predictions were generated using two graph DL algorithms—GraphWavenet (GWNet) (Wu et al., 2019) and Spatiotemporal Graph Convolutional Neural Network (STGCN) (Yu et al., 2018), and one traditional DL algorithm – Long Short Term Memory (LSTM). We also employed two baseline algorithms: a traditional neural network algorithm, Multilayer Perceptron (MLP), and a kernel-based algorithm, Spatiotemporal Kernel Density Estimation (STNet-KDE) (Okabe et al., 2009). For hyperparameter tuning, we followed a two-step procedure that optimizes data representation: train window (i.e., historical period used for prediction), smoothing factor (i.e., temporal decay of past crimes), spatial bandwidth (i.e., spatial influence range), and model parameters: learning rate (i.e., model update speed) for each algorithm. In the final step, we performed a comparative performance analysis between models using the Mean Hit Rate (MHR) metric, which indicates the average percentage of captured events throughout the test period. We tested the significance of the differences in predictive performance across the models with the Wilcoxon signed-rank test.

The current study contributes to existing literature in three significant ways:

- It introduces two novel network-based dynamic crime risk scores, LRS and SSRS, designed to enhance predictions in PCHMs on street networks.
- It incorporates these developed scores into the various PCHM algorithms as dy-

namic features.
- It outlines a two-step hyperparameter tuning procedure that sequentially optimizes both data representation and model performance for the selected DL algorithms.

Related Work

Predicting Crime Hotspots

Crime is not evenly distributed across spaces but is highly concentrated in minimal number of areas known as hotspots (Sherman et al., 1989; Weisburd, 2015; Al-Sabbagh et al., 2024). This well-established fact has led to the development of hotspot policing strategies, which aim to reduce crime rates by deploying law enforcement agents to the existing hotspots (Sherman & Weisburd, 1995; Ariel & Partridge 2017). Although these strategies perform acceptably in many cases, they are reactive and often fail to address the displacement and diffusion of crime hotspots (Repetto, 1976). Alternatively, prospective methods predict future crime hotspots based on past incidents across a region. These methods are based on the boost hypothesis, which suggests that initial victimization enhances a place's vulnerability to subsequent crime (Bowers et al., 2004; Johnson & Bowers, 2004). Subsequent crimes in these locations are often committed by the same offenders, who return to places where they have previously succeeded. This pattern elevates crime risk in these areas for a certain period (Bowers et al., 2004), manifesting as repeat and near-repeat victimization patterns (Pease, 1998; Farrel & Pease, 2001). A significant amount of research supports this hypothesis, especially for acquisitive crimes like burglary (Bernasco & Nieuwbeerta, 2005; Vandeviver et al., 2023).

Johnson and Bowers (2004) explain this behavior through Optimal Foraging Theory (OFT), which suggests that offenders, like foragers, aim to maximize rewards while minimizing risk and effort (Cornish & Clarke, 1987). With each successful offense, the offender gains experience and competence, which enhances their operational effectiveness within known areas. Accordingly, constructing a spatiotemporal risk buffer around crime locations facilitates the creation of hotspot maps that depict areas with the highest crime risk during a specific period (Groff & La Vigne, 2002). In general, this approach underpins PCHM that generates a risk surface where each unit (regular-sized grids) is represented with a crime risk intensity, calculated by a function that inversely weighs the time elapsed and the distance from the unit's centroid. To date, researchers have proposed various PCHM techniques, such as Kernel Density Estimation (KDE) (Bowers et al., 2004) and the Self-Exciting Point Process (SEPP) (Mohler et al., 2011). More recently, Rosser et al. (2017) developed an alternative PCHM technique called NetworkKDE, which operates within a network-constrained space. The authors reported significantly superior predictive performance for this method compared to its grid-based counterparts. This research is pivotal as it was the first to adapt PCHM to street networks, providing a compelling argument for adopting network-based units.

However, the boost hypothesis is not the only perspective that explains spatiotemporal crime patterns. Alternatively, but not contrastingly, the flag hypothesis shifts focus from the offender to the target, highlighting why certain targets are more appealing and thus more susceptible to crime (Johnson & Bowers, 2004). Areas with a higher concentration of these attractive targets offer more opportunities for crime, making them key focal points for offenders (Brantingham & Brantingham, 1981;1995). Understanding why offenders are drawn to specific targets can significantly elucidate what intensifies a hotspot (Groff & La Vigne, 2002). Therefore, integrating the boost hypothesis with the flag hypothesis appears to be a promising direction in PCHM, as supported by prior research (Bernasco, 2010). Incorporating theory-based indicators of target attractiveness could be a valuable first step towards achieving this integration.

Spatial Influence

Incorporating contextual indicators can enhance PCHMs by improving the ability to anticipate changes in crime patterns. One notable set of indicators derives from crime opportunity theories. Rational Activity Theory (RAT) conceptualizes an opportunity for crime as the spatiotemporal convergence of a suitable target and a motivated offender in the absence of a capable guardian (Cohen & Felson, 1979). Extending this concept, Crime Pattern Theory (CPT) (Brantingham & Brantingham, 1981;1995) posits that offenders interpret these opportunities through the mental templates of their familiar environments. These templates are shaped by areas they frequently traverse, typically via street networks, where they assess potential risks and rewards of opportunities (Cornish & Clarke, 1987). A key research question has been why offenders consistently prefer certain locations (Bernasco & Nieuwbeerta, 2005; Bernasco, 2010). CPT offers a compelling explanation by categorizing urban features into two types: crime attractors and crime generators. Crime attractors draw large crowds, raising the probability that suitable targets will encounter motivated offenders, while crime generators have inherent characteristics that facilitate criminal activities. Empirical research has confirmed the significant spatial influence of these features on nearby crime (Ratcliffe, 2012; Groff, 2011; Groff & Lockwood, 2014). Human activity serves as a crucial factor in spatial influence: the more active an area, the greater its influence (Groff, 2011). Temporal constraints also shape this activity, as seen in daily and weekly patterns. For instance, business districts are bustling during work hours on weekdays, while increased activity tends to shift to public transit and grocery stores in the evenings. Conversely, on weekends, these districts quiet down as people typically relax at home or socialize in entertainment areas. The temporal instability of these influences—varying throughout the day (Habermann & Ratcliffe, 2015) and week (Drawve, 2016)—highlights the dynamic nature of crime patterns. Additionally, the situational perspective emphasizes that the spatial influence of crime also varies by type, influenced by the associated risks and rewards (Drawve, 2016). In summary, an effective risk indicator must accommodate these spatial and temporal dimensions from the perspectives outlined.

One remarkable crime prediction method that incorporates spatial influence is Risk Terrain Modeling (RTM) (Caplan et al., 2011). This method aggregates expo-

sure-related factors, such as crime density, with vulnerability-related factors, such as the count of criminogenic urban features, within grids to calculate a risk score. This score identifies potential hotspots for upcoming periods. Numerous studies have highlighted the predictive superiority of RTM over other crime hotspot prediction techniques (Drawve, 2016; Ohyama & Amemiya, 2018). In a different approach, recent researchers (Hakyemez & Badur, 2021) have developed a technique called the Distance-Aware Risk Signal Function (DRSF). This method models the dynamic spatial impact of urban features on fluctuating crime risks within a defined network bandwidth. Analogous to a base station, it conceptualizes urban features as 'crime risk stations' that emit dynamic crime risk signals across street networks. These signals represent the cumulative crime density within a given bandwidth and vary according to different spatial, temporal, and crime-type configurations. The study reported significant spatiotemporal differences in crime risk across types, indicating a dynamic spatial influence of urban features on crime. Such dynamic risk indicators could be instrumental in informing PCHM methods by identifying riskier environmental settings across cities for given periods.

DL-based Crime Hotspot Prediction

Predicting future crime hotspots using machine learning techniques is well-established in the field, with research extending over the past three decades (Olligschlaeger, 1997; Corcoran et al., 2003). Historically, these predictions have utilized traditional machine learning algorithms, including Artificial Neural Networks (ANN), Support Vector Machines (SVM), logistic regression, and ensemble methods (Kadar et al., 2019; Rummens, Hardyns, & Pauwels, 2017). More recently, Deep Learning (DL) algorithms have been incorporated, significantly enhancing the capabilities for crime hotspot prediction (Zhuang et al., 2017; Safat et al., 2021). Commonly, these studies involve dividing a geographic area into a series of equally-sized grids and aggregating potential covariates, such as municipality service calls and points of interest (POI), within these grids. However, as previously discussed in the introduction, this method poses several problems, particularly in how it handles network-constrained crime risk and selects suitable grid sizes.

Recently, street segments have been identified as the ideal geographical unit for crime research because they balance the need for capturing spatial variations with minimizing geocoding errors (Weisburd et al., 2012). In response to the need for placing crime data accurately on street networks, researchers have increasingly turned to spatiotemporal graph learning algorithms for predicting crime hotspots. These methods have shown superiority over traditional Deep Learning (DL) algorithms (Jin et al., 2022, 2023; Hou et al., 2022; Wang et al., 2022). The advantage of graph learning algorithms is their capacity to model spatiotemporal dependencies among neighboring nodes (i.e., street segments) within graphs (i.e., street networks). This capability is essential due to the spatiotemporal diffusion effect observed in crime patterns (Johnson & Bowers, 2004; Pitcher & Johnson, 2011), which indicates that crime is more likely to occur near previous crime locations within a specific timeframe. Effectively capturing this spatiotemporal regularity is critical to the performance superiority reported in these studies.

Similar to the approach adopted in this study, Zhang and Cheng (2020) proposed a DL method that translates PCHM as a task of graph learning. To do this, they proposed the creation of a graph where the midpoints of street segments represent nodes. In this graph, they used a Gaussian kernel weighting function to weight the edges inversely related to the network distance between two nodes. To tackle the challenge of sparse datasets in deep learning (DL), they proposed smoothing crime counts within segments to make them compatible with graph-based DL models. They then interpreted these smoothed counts as graph signals, enabling their use with graph learning algorithms. This adaptation has rendered graph learning algorithms suitable for Predictive Crime Hotspot Mapping (PCHM). However, enhancement through theory-based covariates has not been tested in the existing research except for a few studies (Hakyemez & Badur, 2023). In sum, it can be argued that the applicability of graph learning algorithms to PCHM appears to remain underexplored in the existing research.

This Study

The current study aligns with research utilizing DL algorithms for PCHM on street networks. While most existing methods predict hotspots using historical crime data, typically underpinned by the boost hypothesis—which posits that an initial crime may trigger subsequent nearby crimes for a brief period—our approach innovatively introduces a theory-based risk score, the Street Segment Risk Score (SSRS). This score dynamically captures the crime risks of street segments throughout the day and week. Our method could be seen as an integration of the flag hypothesis with the boost hypothesis, linking the attractiveness of targets to offenders' choices. Linking these hypotheses is a worthwhile endeavour not because it captures dynamic environmental risk, but because it shows how offenders adjust their risk-and-reward perceptions over time and across places and crime types.

The operationalization of target attractiveness is informed by crime opportunity theories- Routine Activity Theory (RAT), Rational Choice Theory (RCT), and Crime Pattern Theory (CPT). The first explains how crime occurs from a spatiotemporal perspective; the second adds a psychological lens on the circumstances under which offenders become more motivated; and the third offers invaluable insights into urban crime, focusing on social interactions among city dwellers. To quantify the attractiveness of places (i.e., street segments), we employ Distance-Aware Risk Signal Functions (DRSFs) (Hakyemez & Badur, 2021), tailored across both daily and weekly models. Specifically, we fit five different DRSFs—three for intraday and two for weekly models—customized for each crime type and urban feature pairing. From these functions, we derive Local Risk Scores (LRS), a novel metric measuring the local effects (i.e., cumulative crime density) of urban features on crime within a street segment. The overall SSRS is produced by multiplying the LRS values for each feature, a method justified by the spatial interaction between nearby urban features, such as the elevated crime risk around a pub in the presence of a nearby liquor store (Block & Block, 1995). Such spatial interactions have been well documented in previous research (Hart & Miethe, 2015; Summers & Caballero, 2017; Yue et al., 2017). An important addition to the SSRS is that it accounts for both vulnerability—the inher-

ent likelihood of crime occurring around specific places—and exposure, meaning the realized vulnerability as indicated by the level of crime concentration around those places (Kennedy et al., 2016). As a result, SSRS can differentiate risk levels between two street segments located in different regions of a city, say one on the Center Side and one on the South Side of Chicago, even if they have identical urban feature compositions. For example, two segments that both contain a pub and a bus stop may receive different SSRS values depending on their location within the city, as the score incorporates each segment's actual exposure to crime.

The SSRS is then utilized to create an auxiliary risk surface, capturing the dynamic crime risk across street segments and integrating it into various PCHM methods using various deep learning, particularly graph learning, algorithms. The reason behind the usage of graph learning algorithms is that graph models keep the connections between places (rather than flattening them), they tend to predict urban crime patterns more accurately than simple pooling methods (Bronstein et al., 2021).A significant contribution of this study is the two-step hyperparameter tuning procedure that sequentially optimizes data representation and model parameters for the employed DL algorithms. In summary, this research proposes a network-based dynamic crime risk surface to enhance the predictive accuracy of PCHM methods.

Methodology

Study Setting

Chicago, IL, the third-largest city in the U.S., boasts a population of nearly 3 million. The city is organized into various geographical units, including 200 neighborhoods, 77 community areas, and nine sides, which function as administrative districts. There exists a clear hierarchical relationship among these units: each neighborhood is part of a single community area, which in turn belongs to one of the nine sides. Prior research has documented significant variabilities in crime rates across these sides (Hakyemez & Badur, 2021; Rosser & Cheng, 2019). Our study focuses on the Central Side (CS), which includes three community areas: Near North Side, The Loop, and Near South Side. This side encompasses downtown Chicago, housing the main business and entertainment districts, as well as numerous historical sites. The CS serves as a critical functional urban area, facilitating employment opportunities and intense social interactions and serving as an entertainment hub. These factors contribute to its distinctive crime dynamics.

During the 2014–2019 period, the five-year crime rate per 1,000 persons on the CS was 466.65, significantly higher than the city average of 374.86. For the crime types selected for our analysis, robbery, and theft, the figures on the CS stood at 18.10 and 300.43, respectively. While the robbery rate was slightly below the city average of 19.58, the rate of theft was considerably higher than the city average of 113.70. The study area is illustrated in Fig. 1.

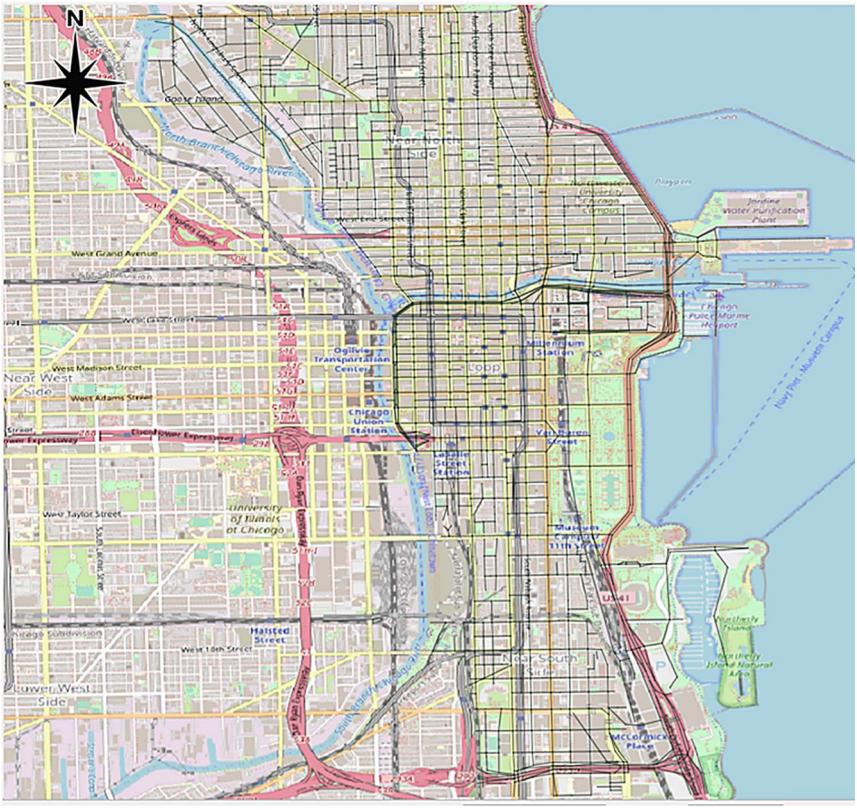

Fig. 1 Street network map of central side of Chicago

Crime Data

We retrieved a sample from the publicly available Chicago crime dataset hosted on the City of Chicago Data Portal. Our analysis focused on two separate samples covering reported incidents of robbery and theft in the Central Side (CS) from 2015 to 2018. The first dataset included 8,897 theft and 461 robbery incidents from 2015. This data was utilized to fit individual Distance-Aware Risk Signal Functions (DRSFs) for each selected urban feature across two temporal levels: intraday and weekly. At the intraday level, incidents were allocated to one of three equal shifts during the day, based on the hour of occurrence. These shifts correspond to the working watches of Chicago police officers (Chicago Police Department., 2021) and are as follows: the first shift (FS) from 00:00 to 07:59, the second shift (SS) from 08:00 to 15:59, and the third shift (TS) from 16:00 to 23:59. At the weekly level, incidents were categorized into weekend (WE) and weekday (WD) groups. The weekend category encompassed all incidents from the third shift of Friday to the first shift of Monday (excluding Monday), while the weekday category included the remaining incidents. The second dataset was subsequently used to implement our Deep Learning (DL)-based crime hotspot prediction This dataset includes all the robbery ($n=1555$) and

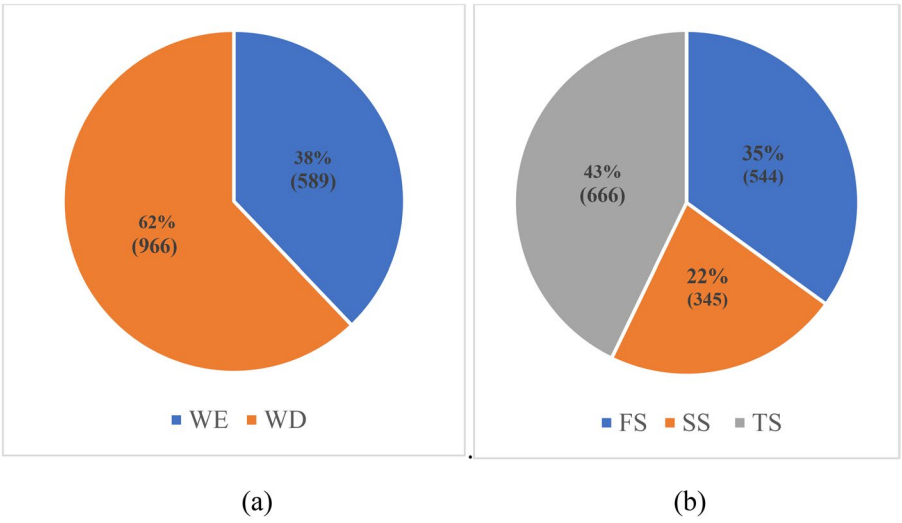

Fig. 2 **a** Weekly and **b** daily distribution of robbery incidents

theft ($n=22596$) incidents reported on the CS between 1st January 2016 and 31st December 2017. The temporal crime distributions are displayed in Figs. 2 and 3.

Urban Features Location Data

In this study, we selected a representative sample of urban features consistently reported to have a significant spatial influence on crime, according to studies focused on Chicago (Bernasco et al., 2017; Bernasco & Block, 2011; Barnum et al., 2017;

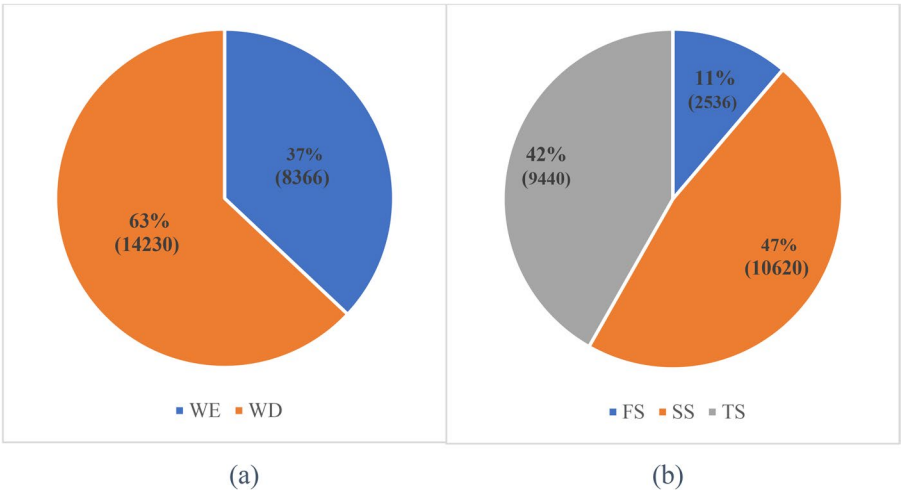

Fig. 3 **a** Weekly and **b** daily distribution of theft incidents

Bernasco & Block, 2009; Kennedy et al., 2016). These features include bus stops ($n=509$), fast food restaurants ($n=70$), gas stations ($n=8$), grocery stores ($n=142$), and pubs ($n=139$). We sourced the locations of these features from two different datasets. First, the locations of businesses such as fast-food restaurants, gas stations, grocery stores, and pubs were obtained from the business license dataset available on the City of Chicago Data Portal. To ensure the uniqueness of the dataset, we eliminated records that belonged to the same applicant at the same location and selected unique locations based on the business activity definitions included in the dataset. Second, the locations of bus stops were retrieved from the CTA bus stops shapefile, also available on the City of Chicago Data Portal. The spatial distribution of these selected features across the Central Side (CS) is depicted in Fig. 4.

Analytical Framework

The methodology begins by fitting five separate DRSFs for each crime type—robbery and theft—and for each urban feature pair (bus stops, fast food restaurants, grocery stores, and pubs). These functions are fitted at two temporal aggregation levels: intraday (First Shift (FS): 00:00–07:59, Second Shift (SS): 08:00–15:59, and Third Shift (TS): 16:00–23:59) and weekly (weekday vs. weekend). Next, crime-specific Local Risk Scores (LRS) for each pair are derived by evaluating the related DRSF at the exact location of each urban feature. These values are then aggregated at the street segment level by multiplication to form the Street Segment Risk Score (SSRS). Using these SSRS values, we created an auxiliary risk surface, representing each street segment by its respective SSRS value for the current period. To evaluate the effectiveness of the SSRS-based risk surface, we also generated another surface based solely on the count of selected urban features within each segment. In the second step, we incorporated these developed risk surfaces—SSRS and feature counts—into various Predictive Crime Hotspot Mapping (PCHM) methods using two graph learning algorithms, GWNet (Wu et al., 2019) and STGCN (Yu et al., 2018), a traditional DL algorithm, LSTM. We developed twelve crime prediction models for each algorithm, generating daily and intraday predictions, both with and without auxiliary risk surfaces. Model performance was assessed using the Mean Hit Rate (MHR) (Zhang & Cheng, 2020), which denotes the average percentage of accurately predicted crime

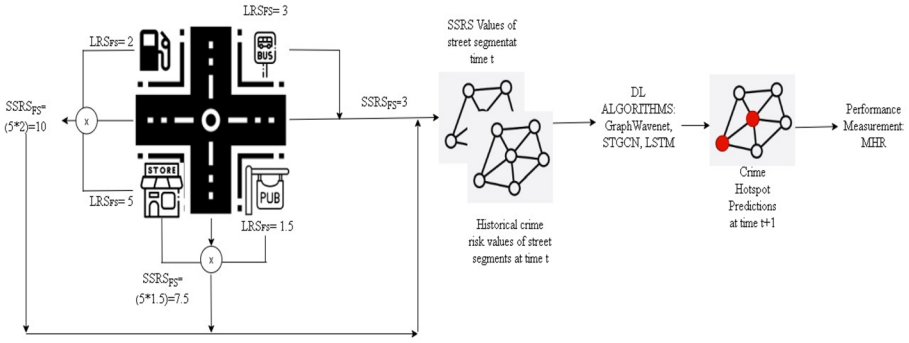

Fig. 4 Incorporating SSRS into DL-based crime hotspot predictions

incidents within a geographical area during a test period. Following this, a two-step procedure for hyperparameter tuning was implemented to sequentially optimize data representation and model parameters. For comparison with deep learning (DL) algorithms, we implemented Multilayer Perceptron (MLP) and Spatiotemporal Network Kernel Density Estimation (STNetKDE) as two baseline models to both demonstrate the effectiveness of the proposed score and assess the performance of the selected DL algorithms relative to their traditional counterparts. We conducted a simple hyperparameter tuning process, experimenting with training window sizes of 21, 42, and 100 timesteps. A training window of 21 timesteps consistently produced the best MHR results across all models and was thus selected. Additionally, a smoothing coefficient of 0.1 was applied to all MLP models. There were three key parameters for the STNetKDE: spatial bandwidth, train window, and smoothing factor. Several experiments produced the following optimal values: 3 for spatial bandwidth (moderate influence on neighboring segments), 10 days or 30 shifts for the train window, and 0.3 for the smoothing factor (moderate temporal decay).

Finally, a comparative performance analysis was conducted among the various crime hotspot prediction models developed. The significance of the performance differences among these models was examined using the Wilcoxon signed-rank test. Lastly, Fig. 5 illustrates a sample process of incorporating SSRS during the first shift (FS) into crime hotspot predictions.

Creating the Individual Street Network for the CS

We utilized the 'Street Centerlines and Boundaries - Community Areas' shapefile available on the Chicago Data Portal for our spatial analysis. The first shapefile con-

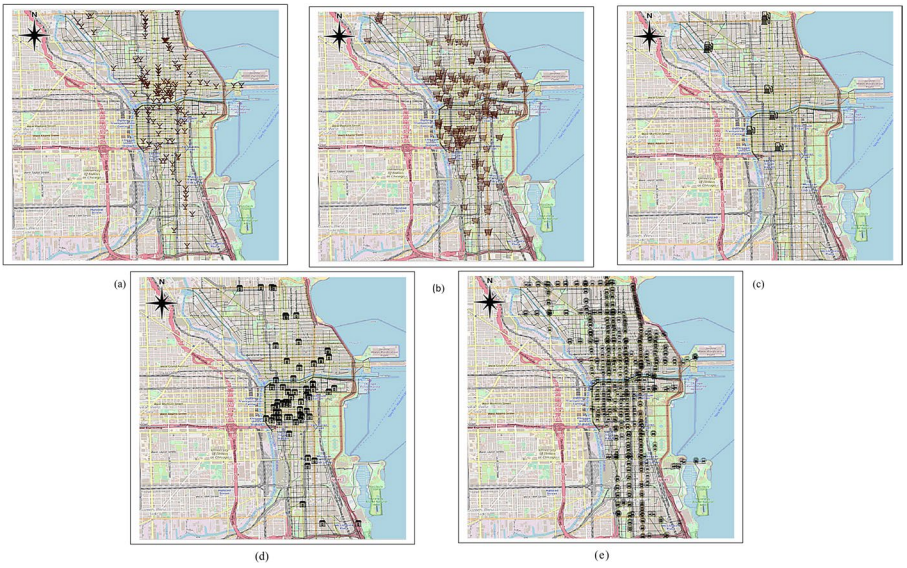

Fig. 5 The spatial distribution of the selected urban features: a Pub b Grocery store c Gas station d Fast food restaurant e bus stop

tains street segment records, detailing attributes such as segment ID, intersection IDs, GPS coordinates of the intersections, and segment length. We joined these segments to the nearest community areas as defined in the second shapefile, using the NNQGIS plugin in QGIS 3.6.0 software. This procedure mapped segments to corresponding community areas and created distinct networks. We filtered the segments to include only those mapped to community areas within the CS: The Loop, Near North Side, and Near South Side. Using the 'spatstat' package in R (Baddeley & Turner, 2005), we identified independent network components and selected the largest one, which contained the highest number of segments, to represent the CS street network. We then excluded all other components and their related segments to prevent distorted network distance calculations (Okabe & Sugihara, 2012). The refined street network consisted of 1,680 nodes (intersections) and 2,459 edges (street segments). Subsequently, we geocoded all reported robbery and theft incidents from 2015 to 2018 onto this street network. A particular challenge was handling incidents that did not fall directly on the created network. To address this, we employed linear referencing to snap GPS coordinates to the nearest street segment. In line with a dual approach (Zhang & Cheng, 2020), we transformed the network into a network of segments, where nodes represent segment midpoints, and edges denote the network distances between these midpoints. The transformed network comprised 2,459 nodes, corresponding to the street segments. This transformation facilitated the creation of robbery and theft datasets, with each row representing relevant crime counts across the segments (columns) in 8-hour and daily increments.

Calculating SSRS

Distance-aware Risk Signal Functions (DRSF)

A Distance-Aware Risk Signal Function (DRSF) models the spatial influence of an urban feature on crime within a specific network bandwidth (Hakyemez & Badur, 2021). The fitting of DRSFs is accomplished through a two-step methodology that combines Network K analysis with segmented regression. The Network K analysis step is crucial as it filters urban features, retaining only those with a statistically significant spatial influence on nearby crime. Subsequently, segmented regression is employed to model this spatial influence more precisely within the chosen network bandwidth, tailored to specific combinations of spatial setting, time periods, and crime types.

Network K function The Network K function analyzes the spatial association between points of the same or different types that reside on networks. Specifically, in the context of crime analysis, the bivariate Network K function tests whether the spatial distribution of type A points (i.e., crime incidents) is influenced by the spatial distribution of type B points (i.e., urban features). Theoretically, it is formulated as follows

$$\mathbf{K^{ba}(t) = \frac{1}{\rho_a} E(\text{the number of points A within network distance t of a point } b_i \text{ in B})} \quad (1)$$

where E(.) is the expected value of bi, …bn (bi Є B), which follows a binomial point process, and ρ_a is the density of points $\rho_a = \frac{n_a}{|L_T|}$. Here, $|L_T|$ denotes the total length of the line segments in a network. The formula for an observed pattern is:

$$\widehat{K}^{ba}(t) = \frac{|L_T|}{n_a n_b} \sum_{i=1}^{n_b} (\text{the number of points of A on } L_{b_i}(t)) \quad (2)$$

Here, if $\widehat{K}^{ba}(t) > K^{ba}(t)$, then type A points cluster around type B points, else $\widehat{K}^{ba}(t) < K^{ba}(t)$then type A points disperse around type B points. To calculate theoretical $K^{ba}(t)$ involves an analytical approach towards Complete Spatial Randomness (CSR) hypothesis. The CSR hypothesizes that different types of point processes are independently and identically distributed following a binomial distribution on a network space. To test CSR, we run a Monte Carlo simulation that generates 39 random bivariate point patterns of crime and urban features on a network. The minimum and maximum values of $K^{ba}(t)$ in these simulations at a network distance t yield the critical upper and lower values at α=0.05 level (Baddeley et al., 2014). If $\widehat{K}^{ba}(t)$ exceeds the upper value, we can conclude that crime type A points significantly clusters around point B, $\widehat{K}^{ba}(t)$ below the lower value indicates that type A points significantly disperses around point B. Any other values inbetween indicates insignificant spatial relationship. Figure 6 illustrates a sample output of a bivariate network K analysis.

The observed curve in Fig. 6, which runs above the grey belt representing the critical area, indicates a positive clustering of robbery incidents around pubs in the

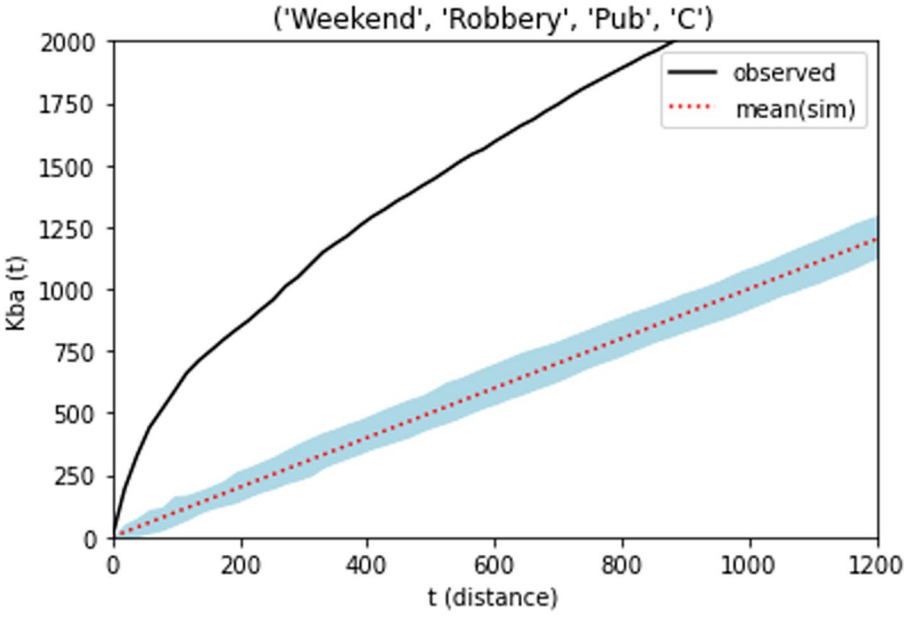

Fig. 6 A sample network K result

Central Side (CS) during weekends. This pattern suggests that the proximity to pubs significantly influences the occurrence of robberies, particularly at these times. In summary, the network K analysis is instrumental in identifying significant crime clusters around specific urban features across street networks, providing valuable insights into spatial dependencies that may inform more targeted crime prevention strategies.

Segmented Regression After identifying urban features with significant spatial influences on nearby crime, we employed segmented regression to fit crime-specific Distance-Aware Risk Signal Functions (DRSFs) across various temporal models. We adopted a quarter-mile (402.4 m) bandwidth, commonly used to delineate the spatial interaction between urban features and crime (Groff, 2011). Segmented regression was utilized to capture the dynamic relationship between crime risk and urban features within this bandwidth. This method fits distinct regression equations for different intervals of an independent variable, each with its own set of coefficients, effectively modeling the changing influence of urban features on crime risk at varying distances (for more details, see Kim et al. (2000)

$$\mathbf{E}[\mathbf{y}|\mathbf{x}] = \boldsymbol{\beta}_0 + \boldsymbol{\beta}_1\mathbf{x} + \boldsymbol{\delta}_1(\mathbf{x} - \boldsymbol{\tau}_1)^+ + \ldots . + \boldsymbol{\delta}_\mathbf{k}(\mathbf{x} - \boldsymbol{\tau}_\mathbf{k})^+ \quad (3)$$

Where $\mathbf{E}[\mathbf{y}|\mathbf{x}]$ represents the expected value of the dependent variable y (i.e., crime risk) at a distance t (x). $\boldsymbol{\tau}_\mathbf{k}$ represents unknown changepoints whereby $(\mathbf{x_i} - \boldsymbol{\tau}_\mathbf{k})^+ = (\mathbf{x_i} - \boldsymbol{\tau}_\mathbf{k})$ if $(\mathbf{x_i} - \boldsymbol{\tau}_\mathbf{k})>0$. $\boldsymbol{\beta}_0$, $\boldsymbol{\beta}_1, \boldsymbol{\delta}_1 \ldots$ $\boldsymbol{\delta}_\mathbf{k}$ are coefficients that were estimated by a permutation test method [71]. The fitted regression model gives the DRSF that shows the changing relationship between crime risk and the distance from an urban feature. This DRSF has the ability to estimate the crime density for any given distance within the specified network bandwidth. Figure 7. illustrates a sample DRSF. For instance, the estimated crime density at 28 m is 3.9; and at 66 m 3.5 approximately.

In this study, we analyzed observations (x_i, y_i) consisting of network distances (x) and corresponding cumulative crime densities (y). For the bivariate network K analysis, we employed the linear K cross function from the spatstat package (Baddeley, 2005) in R. This function computes the observed number of Type A events (i.e., crimes) relative to Type B events (i.e., urban features) at 513 equally spaced points within a bounding radius. This radius is defined as the maximum shortest path distance between any two points on the linear network. For the CS, the bounding box coordinates are set at (41.91, −87.60; 41.84, −87.65), with a bounding radius of 9,977.9 m, resulting in distance chunks of approximately 19.4 m each (9977.9 m/513). To accurately estimate the segmented regression models, we selected an adequate number of observations that cover at least the chosen bandwidth of 402.4 m. Specifically, we used 21 observations, yielding a total coverage of 407.4 m (19.4 m x 21). Using this setup, we fitted separate DRSFs for each configuration—considering the type of urban feature, type of crime, and temporal dimension. This approach allowed us to derive dynamic crime risks across street segments, which were then quantified through the Street Segment Risk Score (SSRS).

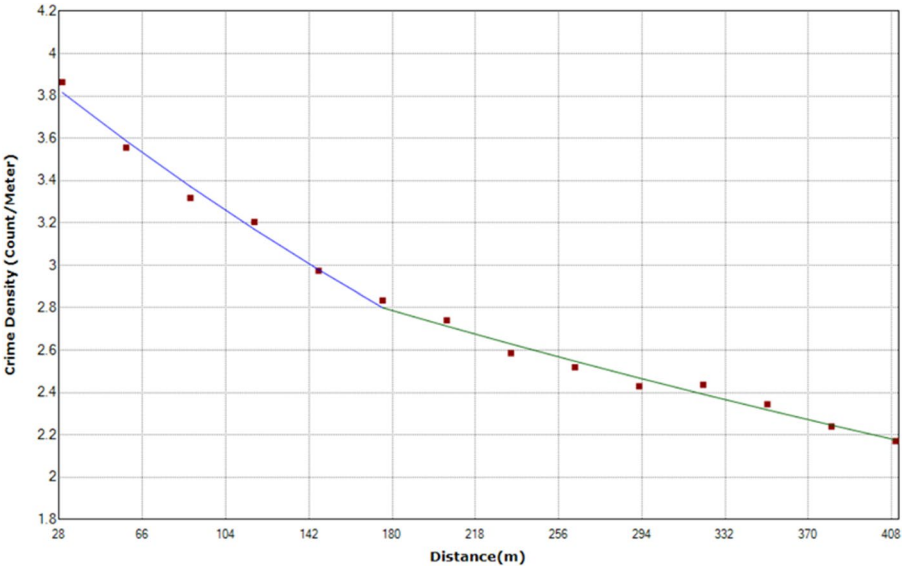

Fig. 7 A sample display of DRSF

LRS and SSRS

The Local Risk Score (LRS) operationalizes the local effect of an urban feature on crime, measured by the value of the corresponding Distance-Aware Risk Signal Function (DRSF) at a distance of 1.7 m (approximately 5.5 feet). This specific bandwidth is used to offset geocoding errors and to isolate crimes that occur directly related to an individual feature (Ratcliffe, 2012). After deriving the LRS values from the DRSFs, we calculate the Street Segment Risk Score (SSRS) for each street segment by multiplying the LRS values of the urban features it hosts. This multiplication approach integrates the spatial interactions between the selected urban features into the prediction models (Hart & Miethe, 2015). For instance, consider a street segment that hosts a grocery store, a gas station, and a pub, with respective LRS values of 3, 4, and 5 during weekdays. The SSRS for theft on this segment would be calculated as $3 \times 4 \times 5 = 60$. On weekends, if the LRS values for the grocery store and pub increase to 4 and 6, and the value for the gas station increases to 7, the SSRS would be $4 \times 6 \times 7 = 168$. It is important to note that we exclude urban features without significant spatial influence from the SSRS calculations. Rather than setting their values to zero—which could result in a zero SSRS due to multiplication—we simply omit these features from the calculation. This approach prevents any potential skewing of the SSRS values to zero. The process of calculating the SSRS is illustrated in Fig. 8.

Formulating Crime Hotspot Prediction Problem

The task of predicting crime hotspots involves identifying the specific times and locations where crimes are likely to occur in the future. In this research, the timeframes are categorized as 'day' and 'shift,' while the spatial units are defined as street

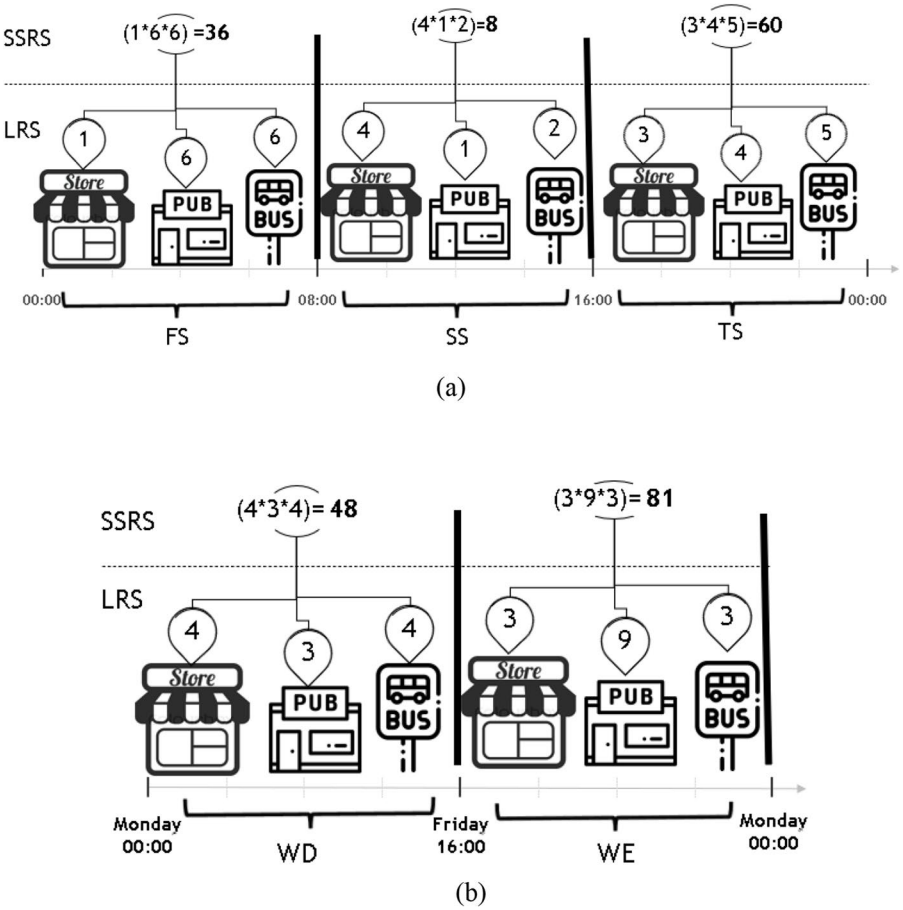

Fig. 8 Calculating SSRS **a** intraday **b** week

segments, which are the sections of a street between two intersections (Weisburd et al., 2012). To predict crime across these segments, a dual approach is employed that transforms street segments into nodes on an undirected graph (Zhang & Cheng, 2020). This method facilitates the analysis and prediction of crime patterns by mapping street segments as interconnected points within a network. $SSRS_{FS}$.

$$G = (V,\ E,\ W) \tag{4}$$

In this context, (G) represents the graph, (V) is the set of nodes, each defined by the midpoints of a street segment, (E) denotes the edges, and (W) represents the inversely weighted network distance between nodes. This inverse weighting embodies the theoretical assumption that spatial dependence diminishes as the distance between nodes increases (Wheeler, 2019). This framework transforms the problem into a graph signal learning task, where the objective is to predict the signals (i.e., crime risk) at each node for the subsequent time step (S). For the multivariate predictions, G has

a dynamic feature matrix $X^{(t)} \varepsilon R^{NXD}$, that represents the covariate(s) (i.e., SSRS and feature counts). Here, N denotes the number of nodes (i.e., street segments), and D is the input dimension.

$$\left[X^{(t-S):t}, G\right] \underset{\rightarrow}{f} X^{(t+1)} \tag{5}$$

Here $X^{(t-S):t} \varepsilon R^{NxDxS}$, and $X^{(t+1)} \varepsilon R^{NxM}$ represent the dynamic feature matrix for the last S time steps, and the prediction matrix in the next step, respectively. M is the output dimension. In short, the problem is to predict crime risk for each segment in the next time step with the provisioned covariate.

Our goal is to predict the likelihood of future crimes on each street segment using past crime data and the Street Segment Risk Score (SSRS). This approach allows us to identify potential crime hotspots more effectively and develop targeted prevention strategies.

Graph Learning Algorithms

GWNet

GWNet (Wu et al., 2019) adapts the Wavenet algorithm (Van Den Oord, 2016) for spatiotemporal graph learning, incorporating two key innovations. The first is a self-adaptive adjacency matrix, which uncovers hidden spatial dependencies by learning node embeddings. The second is a layered dilated 1D convolution component, which captures long-range temporal connections through progressively larger receptive fields in the 1D convolution layers. To address the challenge of learning from sparse sequences in recurrent neural networks, these receptive fields expand exponentially with the increasing number of layers. For more details, refer to Wu et al. (2019).

STGCN

The other graph deep learning algorithm is STGCN (Yu et al., 2018), which models spatiotemporal dependencies using convolutional units exclusively, bypassing recurrent units. It features a design consisting of spatiotemporal convolutional blocks, each containing two gated CNN layers and a graph convolution layer (Defferrard et al., 2016). This architecture effectively captures both temporal dependencies and spatial relationships. Additionally, the use of only convolutional layers results in shorter training times and fewer parameters. For more information, refer to Yu et al. (2018).

Loss Function

We overcame the extremely imbalanced datasets in predicting sparse event datasets by developing a squared quantile loss function as suggested by Zhang & Cheng (2020). This function heavily penalizes underpredictions in that the primary objective in a crime prediction is to predict nonzero cases (i.e., crime events). In other words, the cost of a false negative (i.e., missing a crime event) should be significantly higher

than the cost of a false positive (i.e., overprediction). Accordingly, we formulated our weighted loss function as follows:

$$loss = \frac{1}{N} \sum {}^{N}_{i=0} w_i (\widehat{y}_i - y_i)^2 \tag{6}$$

Here, $\widehat{y}_i$ and y_i are predicted and actual values respectively. w_i is an asymmetric weight changing based on the value of y_i. Similar to a quantile loss function, we formulated this weight as:

$$w_i = \begin{cases} q \; if \; y_i > 0 \\ (1-q) \; if \; y_i = 0 \end{cases} \tag{7}$$

Here q ϵ [0,1] is a coefficient. For larger values, it severely penalizes underpredictions, which corresponds to missing a crime event. This function helps the selected algorithms focus on predicting rare crime events by sharpening the contrast between the costs of missing zero and nonzero observations. For example, setting the q value at 0.95 penalizes the underpredictions 19 times higher than that applied to overpredictions.

Performance Measurement

The performance of the selected algorithms was assessed using the MHR (Mean Hit Rate) metric. This metric calculates the average percentage of crimes occurring in predicted hotspots (i.e., street segments) on test days. The evaluation process involves the following steps:

1. **Sorting**: Street segments are sorted in descending order based on their predicted crime risk values for each time step.
2. **Selection**: Segments are selected from the top of the list such that their total length does not exceed the specified coverage area. This coverage area represents the allowable percentage of the total length of street segments designated to predict crime hotspots, ensuring specificity in predictions.
3. **Calculation**: For each time step, the number of crime incidents occurring in the selected segments is divided by the total number of incidents across all segments. This value is then multiplied by 100 to obtain the Hit Rate (HR).
4. **Averaging**: The average HR across test days is computed to determine the MHR.

For example, an MHR of 80% at a 10% coverage area indicates that, on average, 80% of crime events occurred in the predicted hotspots (i.e., segments) that account for 10% of the total length of street segments for each time step. An MHR plot shows how performance varies across different coverage values, displaying MHR values corresponding to coverage areas ranging from 1% to 20% in 1% increments. Figure 9 illustrates a daily PCHM for theft incidents on the first day of the testing period (i.e., May 27, 2025). Segments highlighted in blue represent the predicted hotspots (i.e., 464 segments out of 2459) based on daily predictions generated by GWNet

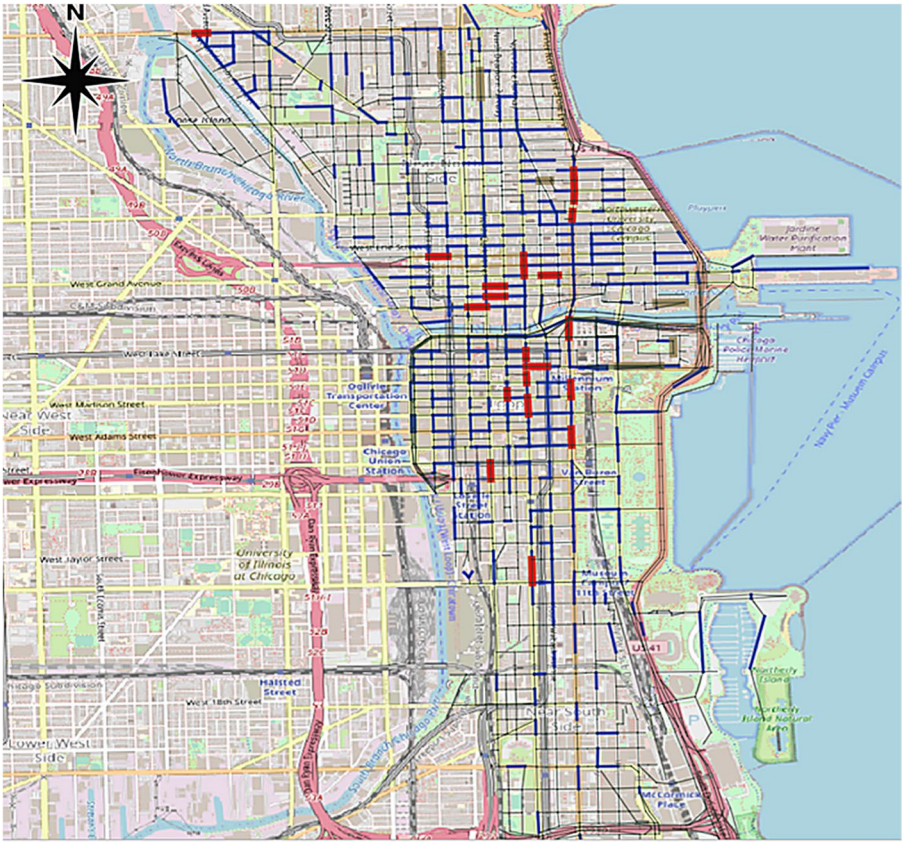

Fig. 9 A sample PCHM illustration

with SSRS. Segments highlighted in red indicate predicted hotspots where theft incidents actually occurred (i.e., hit cases), while black segments represent actual crime incidents that occurred outside the predicted hotspots (i.e., miss cases). On this day, 29 theft incidents were recorded in the CS area of Chicago. The predicted hotspots captured 23 of these incidents, resulting in a hit rate of 79.31% for a coverage area of 20%.

Experiments

In the first step of our two-step hyperparameter tuning procedure, we investigated three parameters related to data representation: the time window, smoothing coefficient, and spatial bandwidth. The time window determines the number of previous time steps used to predict the next one, while the smoothing coefficient and spatial bandwidth adjust the temporal and spatial extent of risk following a crime event. We tested all possible combinations of these parameters (i.e., time window x smoothing coefficient x spatial bandwidth), resulting in 60 configurations for daily models and

Table 1 The experimental setup

	Daily	Shift
Data representation		
Train window	7,10,14,30,42	3,21,30,42
Smoothing coefficients	0.05, 0.1, 0.5, 0.9	
Spatial bandwidth	0.1, 0.2, 0.3	
Model		
Learning rate (ρ)	0.001,0.01,0.02,0.03,0.04,0.05,0.06,0.07,0.08,0.09,0.1	

48 configurations for shift models. We selected the configuration with the highest MHR at 20% coverage as the optimal data representation.

In the second step, using this optimal representation, we tested 11 different values for the learning rate (ρ), which controls the rate of convergence in minimizing the loss function. This parameter is often cited as crucial in the hyperparameter tuning of deep learning algorithms (Bengio, 2012). We repeated this process for each selected crime type (i.e., Robbery, Theft) and temporal level (i.e., daily and shift). The values experimented with in each step are detailed in Table 1 below, while Table 2 reports the key architectural parameters of the selected deep learning algorithms.

Here, "patience" refers to the number of epochs we waited to observe changes in weights. For example, we terminated models if no weight changes occurred over 25 consecutive steps, using this parameter as a stopping criterion. The batch size was determined by the maximum number of instances that could be included in each batch. For the optimizers, we tested various types and selected those that achieved the best MHRs.

For daily models, the dataset includes 730 daily observations from January 1, 2016, to December 31, 2017. The training set comprises the first 511 days (January 1, 2016, to May 26, 2017), the validation set covers the next 73 days (May 27, 2017, to August 8, 2017), and the test set includes the final 146 days (August 9, 2017, to December 31, 2017). For shift models, the dataset consists of 2,190 observations (730×3). Similarly, we used the first 1,533 observations for training, 219 for validation, and 438 for testing.

Testing the Significance of the Performance Differences between the Models

To test the effectiveness of the risk surfaces developed (i.e., SSRS and feature counts), we performed a Wilcoxon signed-rank test on the 20 MHR values reported at each coverage area from 1% to 20%. Since we assumed the predictive value of these surfaces, we tested left one-tailed hypothesis ($\alpha = 0.025$) where:

Table 2 Key architectural parameters of the selected DL algorithms

Algorithm	Epochs	Patience	Batch Size	Optimizer	Split (%)
GWNet	100	25	16	Adam	70-10–20
STGCN	100	25	8	Adam	70-10–20
LSTM	100	25	16	RMSProp	70-10–20
MLP	100	-	16	Adam	70-10–20

$$H_0 : MHR_{prospective} = MHR_{withauxiliaryrisksurface} \quad (8)$$

$$H_1 : MHR_{prospective} < MHR_{withauxiliaryrisksurface} \quad (9)$$

Results

SSRS

The main results indicated that pubs have the largest spatial influence on robbery during weekdays, weekends, and the first shift, with LRS values of 4.3, 11.21, and 11.23, respectively. For the second shift and third shift, fast food restaurants replace pubs with LRS values of 4.49 and 7.23, respectively. Another important result is that gas stations do not have a significant spatial influence on robbery across street segments. The detailed LRS results are displayed in Fig. 10.

For theft incidents, we found the largest spatial influence, as operationalized by LRS, values around pubs across all temporal models. The fast-food restaurants and grocery stores come second across different temporal levels. While fast food restaurants have the largest LRS values during weekdays (WD) and first shift (FS) with LRS values of 4.13 and 5.37, grocery store is the urban feature having the second largest LRS values across weekend (WE) (LRS = 4.6), second shift (SS) (LRS = 4.29) and third shift (TS) (LRS = 4.11). In addition, we also do not observe any significant spatial influence of gas station across any temporal levels. The detailed LRS results are displayed in Fig. 11.

Comparative Predictive Performance Analysis

The proposed two-step hyperparameter tuning procedure revealed changing optimal data and model-related parameters across various crime types and temporal levels.

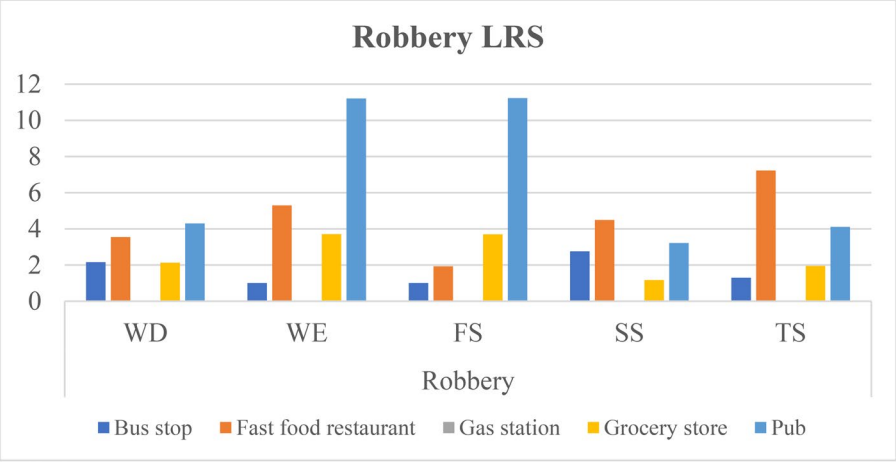

Fig. 10 The robbery LRS values of each urban feature across temporal models

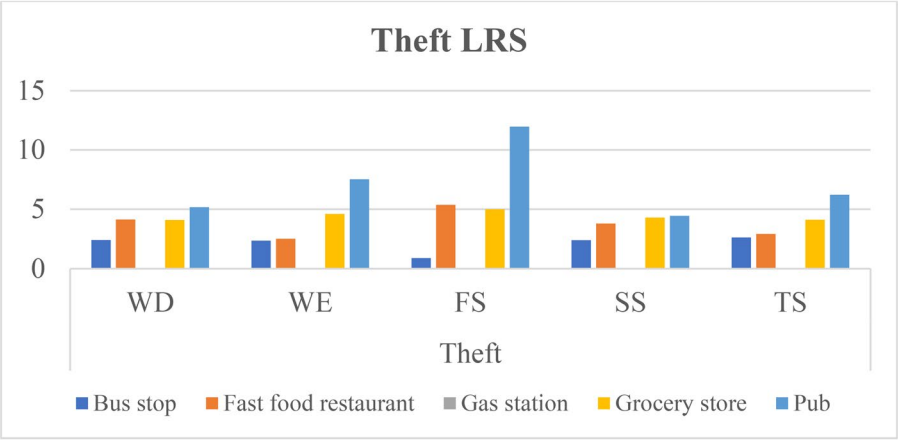

Fig. 11 The theft LRS values of each urban feature across temporal model

Tables 3 and 4, and 5 highlight the differences between different model configurations. The MHR values reported here represent the predictive performance, calculated as the proportion of crime events occurring within the predicted hotspots relative to the total number of events, based on a 20% street segment coverage threshold.

After optimizing each model's parameters, we generated separate MHR plots (Figs. 12a and b and 13a and b). Our key findings demonstrate that incorporating SRSS consistently enhances the performance of all the selected learning algorithms across the majority of the prediction models and crime types. Notably, incorporating SSRS improved robbery shift predictions by up to 65% for the MLP model and up to 92% for the STNetKDE model. Conversely, using feature counts as an auxiliary risk surface negatively impacted performance, reducing shift theft predictions by STGCN by up to 47%.

Importantly, LSTM consistently underperformed compared to graph learning algorithms and MLP, with MHR values between 20 and 30. While MLP's performance was generally inferior to graph learning algorithms, it achieved the highest predictive accuracy for shift theft, with MHRs reaching 79%. A similar observation applies to STNetKDE, which outperforms the remaining algorithms in the theft shift models with an MHR of 66%; however, its performance remains largely inferior to the graph-based learning algorithms and MLP across all other models.

Table 3 The hyperparameter tuning results of prospective robbery and theft models

		Daily					Shift				
Robbery		***TW***	***SC***	***SBW***	***LR***	***MHR(%)***	***TW***	***SC***	***SBW***	***LR***	***MHR(%)***
	GWNet	42	0.05	0.1	0.05	56.2	42	0.05	0.1	0.05	49.5
	STGCN	14	0.05	0.3	0.04	52.8	42	0.9	0.3	0.05	58.4
	LSTM	42	0.5	-	0.01	23.2	3	0.1	-	0.02	22.8
Theft	GWNet	14	0.05	0.2	0.03	76.4	21	0.05	0.3	0.1	59.6
	STGCN	42	0.05	0.1	0.02	77.6	30	0.3	0.3	0.05	56.1
	LSTM	14	0.05	-	0.04	24.5	3	0.9	-	0.04	24.5

TW Train Window, *SC* Smoothing Coefficient, *SBW* Spatial BandWidth, *LR* Learning rate

Table 4 The hyperparameter tuning results of robbery and theft models with SSRS

		Daily					Shift				
Robbery		***TW***	***SC***	***SBW***	***LR***	***MHR(%)***	***TW***	***SC***	***SBW***	***LR***	***MHR(%)***
	GWNet	10	0.1	0.3	0.05	58	3	0.5	0.3	0.07	51.3
	STGCN	30	0.1	0.3	0.02	55.4	30	0.05	0.3	0.08	59.9
	LSTM	30	0.9	-	0.05	23.9	3	0.9	-	0.03	26.7
Theft	GWNet	30	0.05	0.2	0.02	80	3	0.5	0.3	0.02	60.5
	STGCN	14	0.05	0.3	0.06	79.9	30	0.3	0.3	0.04	60.8
	LSTM	14	0.05	-	0.05	24.2	21	0.05	-	0.07	24

TW Train Window, *SC* Smoothing Coefficient, *SBW* Spatial BandWidth, *LR* Learning rate

Table 5 The hyperparameter tuning results of robbery and theft models with feature counts

		Daily					Shift				
Robbery		***TW***	***SC***	***SBW***	***LR***	***MHR(%)***	***TW***	***SC***	***SBW***	***LR***	***MHR(%)***
	GWNet	10	0.9	0.3	0.08	51.4	3	0.1	0.2	0.01	49.6
	STGCN	30	0.05	0.3	0.07	37.4	42	0.05	0.2	0.08	30.9
	LSTM	30	0.5	-	0.04	21.1	3	0.5	-	0.04	23.3
Theft	GWNet	42	0.5	0.2	0.01	68.6	3	0.5	0.2	0.09	50.5
	STGCN	30	0.05	0.3	0.07	53.8	42	0.05	0.2	0.06	60.7
	LSTM	10	0.05	-	0.04	23.2	3.	0.5	-	0.05	22.9

TW Train Window, *SC* Smoothing Coefficient, *SBW* Spatial BandWidth, *LR* Learning rate

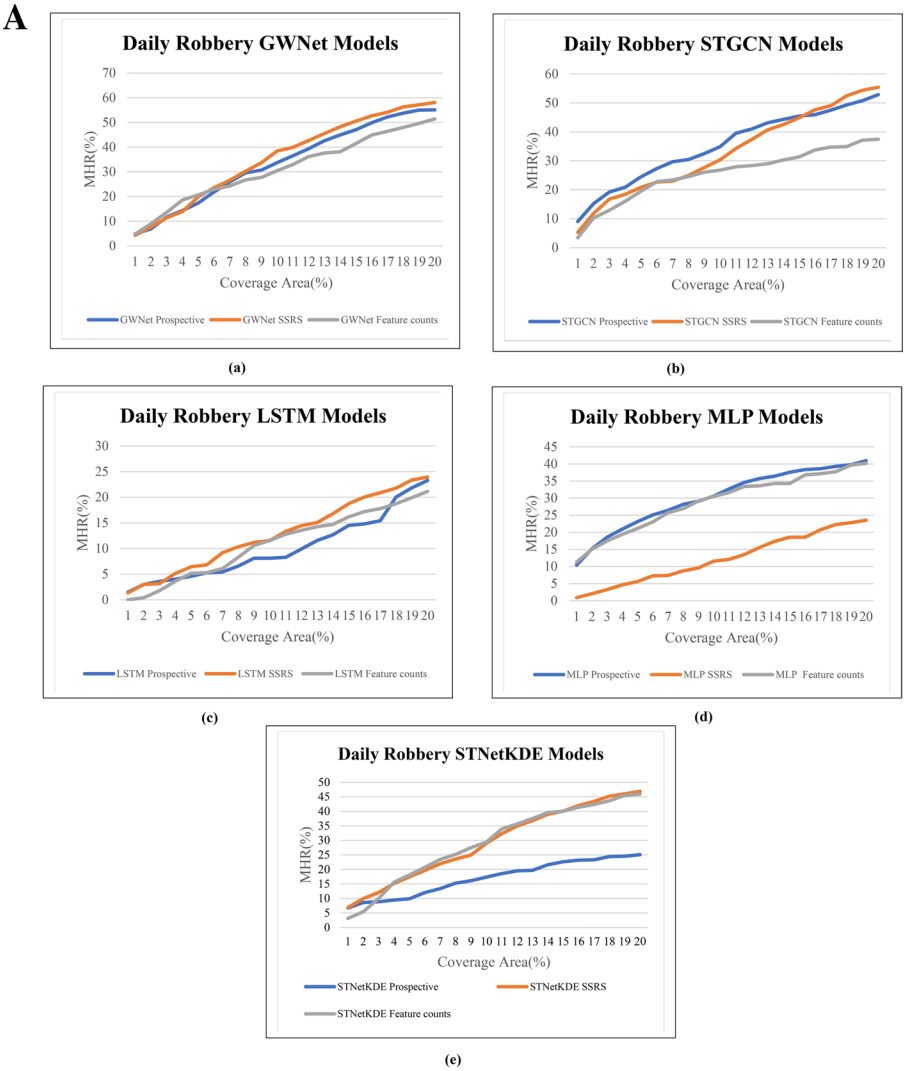

Fig. 12 The MHR plots for daily robbery prediction models **a** GWNet **b** STGCN **c** LSTM **d** MLP **e** STNetKDE

For daily robbery prediction, GWNet with SRSS achieved the best performance with an MHR of 58%. While incorporating SRSS improved STGCN's MHR by 4.8% and GWNet's MHR by 5.3% at 20% coverage area. However, the largest improvement occurred in the performance of STNetKDE with a 87% increase in the MHR value. Conversely, including feature counts negatively impacted performance, decreasing the MHR of LSTM, GWNet, and STGCN by 9%, 6%, and 29%, respectively. In contrast it has a positive impact on the performance of STNetKDE with a 83% increase. Notably, SSRS significantly reduced MLP's MHR from 40% to 23%. For shift-level robbery prediction, STGCN with SRSS performed best

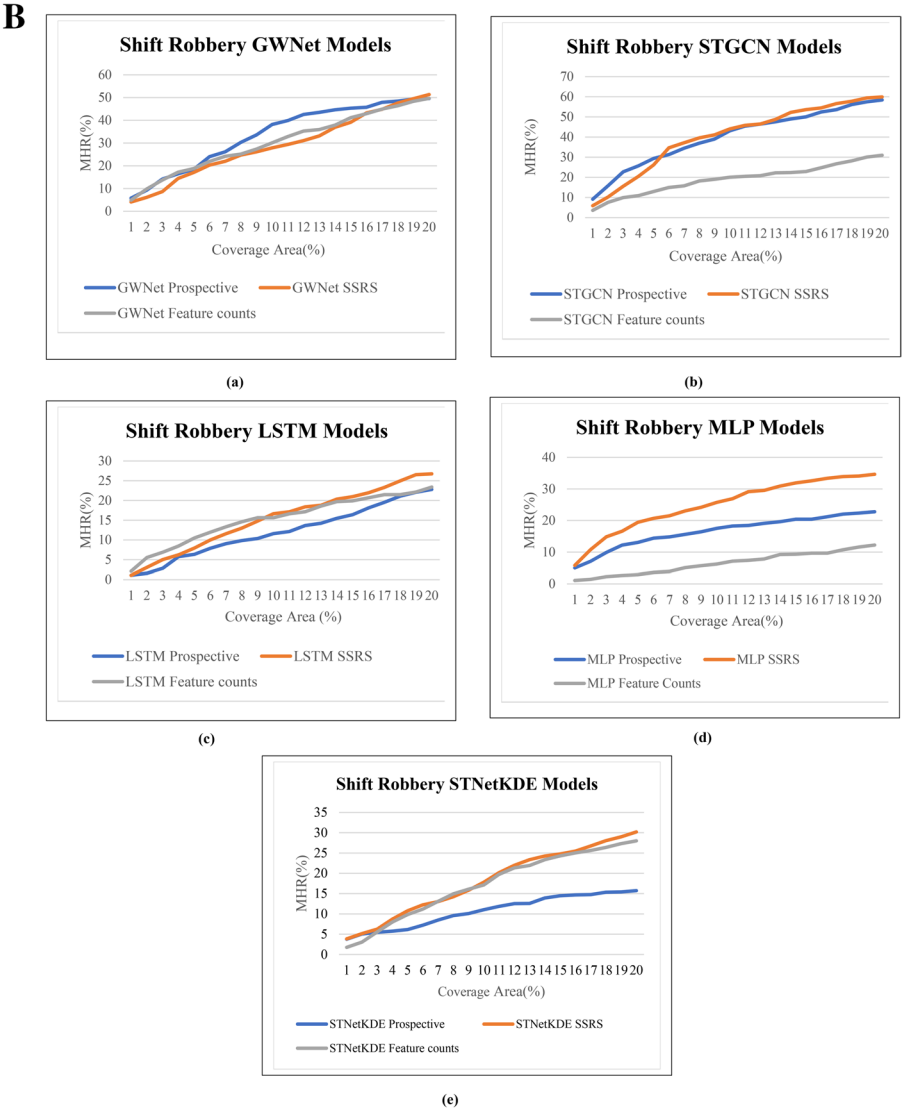

Fig. 12 (continued)

(MHR = 59.9%). Incorporating SRSS consistently improved performance across all algorithms: GWNet (+17%), LSTM (+2.5%), MLP (+33.6%), STNetKDE (92%). Including feature counts slightly improved LSTM, GWNet (by 2.5% and 0.1%) and largely improved STNetKDE (78.1%), but worsened STGCN and MLP (by 47% and 53% respectively).

For daily theft prediction, GWNet with SRSS achieved the highest performance (MHR = 80%), closely followed by STGCN with SRSS (MHR = 79.9%). Incorporating SRSS improved the performance of these graph learning algorithms and STNetKDE by 4.6%, 2.9%, and 11.3%, respectively. However, it decreased the MHR of

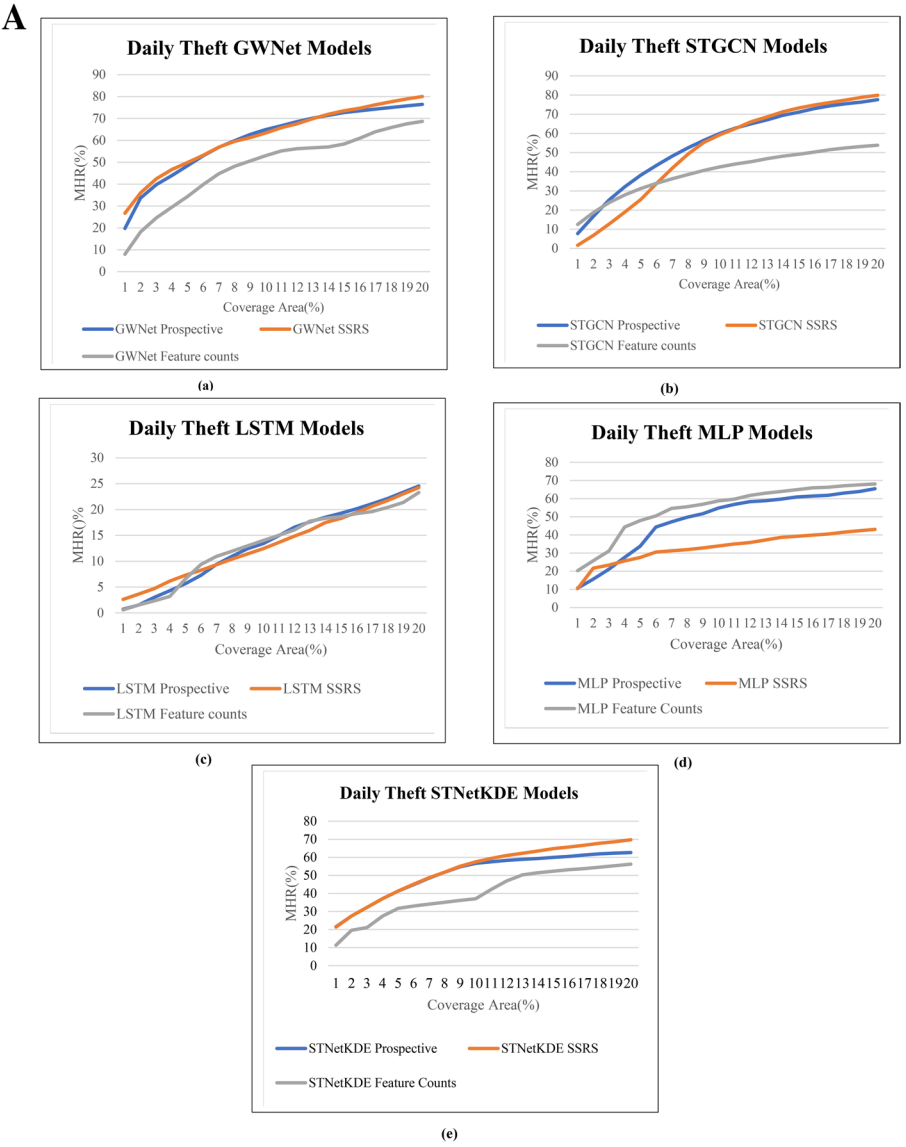

Fig. 13 The MHR plots for daily theft prediction models **a** GWNet **b** STGCN **c** LSTM **d** MLP **e** STNetKDE

LSTM and MLP models by 1% and 34.4%. Adding feature counts further reduced performance across all selected algorithms (GWNet, STGCN, LSTM, STNetKDE) except for MLP, which saw a 4% improvement in MHR. Surprisingly, for shift-level theft prediction, MLP with SRSS outperformed all other models, achieving an MHR of nearly 80%. Even without SRSS, MLP remained the second-best model (MHR = 71.7%). Conversely, incorporating feature counts consistently hindered per-

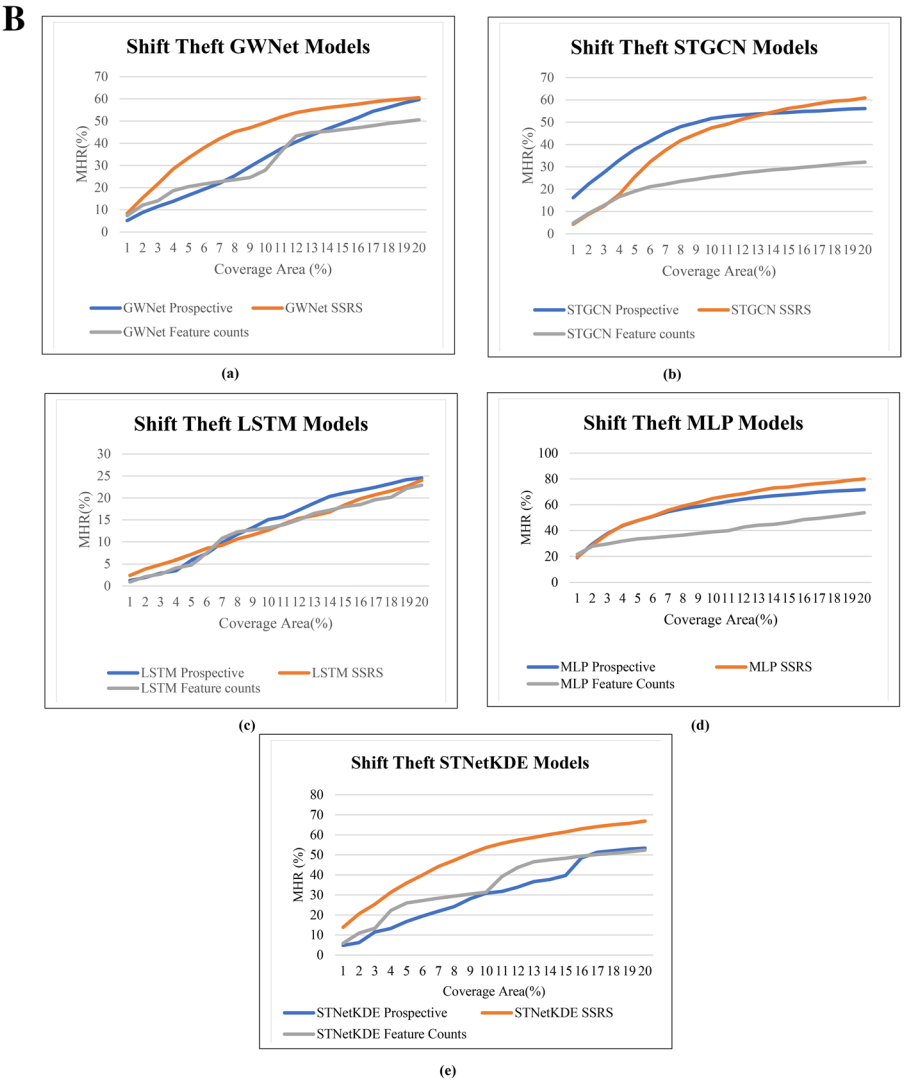

Fig. 13 (continued)

formance, decreasing MHR for LSTM, GWNet, STGCN, MLP, and STNetKDE by 6%, 15%, 42%, 25%, and 7%, respectively.

Finally, the Wilcoxon signed-rank test revealed significant differences in model performance with and without SRSS. Notably, incorporating SRSS significantly improved GWNet's performance across all models except for shift-level robbery hotspot prediction. SRSS also significantly enhanced LSTM's performance in both daily and shift-level robbery prediction. However, no significant improvements were observed for any STGCN hotspot prediction models when incorporating SRSS. For MLP, SRSS significantly improved performance in both robbery and theft shift modelsLastly, STNetKDE demonstrated significantly improved performance when SSRS

and feature counts were incorporated into the prospective model, across all configurations except for the theft daily model that included feature counts.Table 6 below summarizes the hypothesis tests comparing models with and without auxiliary risk surfaces.

Discussion

The LRS results revealed differential weekly and intraday spatial influences of the selected urban features across different crime types, which aligns with the previous research that similarly found supporting evidence for these spatiotemporal crime patterns (Hakyemez & Badur, 2021; Habermann & Ratcliffe, 2015). A striking contrast exists between the pubs and gas stations across the models. While the pubs were found to have the largest influence on robbery during the FS (00:00–07:59) and on theft across all the models, gas stations did not have any influence in any prediction models. A plausible explanation can be derived from Crime Pattern Theory (CPT) (Brantingham & Brantingham, 1981;1995), which conceptualizes crime attractors as environments that facilitate criminal activity due to their distinct spatial characteristics. Similarly, pubs can be considered a type of generator where offenders prefer to operate around pubs late at night, where they are more likely to find intoxicated patrons who may not defend themselves properly (Ratcliffe, 2012). Mostly located near the public transit stations, these places also provide better exit routes for the offenders. On the other hand, gas stations in the CS may be less vulnerable to crime due to their less popular locations or better place management practices (Eck et al., 2007). In either case, caution should be exercised in interpreting these results as the spatial influences of urban features heavily depend on the city context (Kennedy et al., 2016).

The two-step hyperparameter tuning optimization underlines the necessity of a data-driven approach in achieving the optimal data representation for crime prediction. The optimal models were found to have different parameters, training window size, smoothing coefficient, and spatial bandwidth due to changing crime patterns across crime types (Groff & Lockwood, 2014; Grubesic & Mack, 2008). The first two

Table 6 The resulting p-values of Wilcoxon signed rank significance test

p-values		Daily		Shift	
Robbery		**SSRS**	**FC**	**SSRS**	**FC**
	GWNet	**1.3E-05****	0.999	0.999	0.999
	STGCN	0.997570	1.000	0.226	1.00
	LSTM	**1.3E-05****	0.048	**1.9E-06****	**9.5E-07****
	MLP	1.000	1.000	**9.5E-07****	**1**
	STNetKDE	**9.5E-07****	**9.5E-07****	**9.5E-07****	**9.5E-07****
Theft	GWNet	**0.010****	1	**9.5E-07****	0.898
	STGCN	0.891	0.999	0.991	1
	LSTM	0.649	0.795	0.955	0.999
	MLP	1	**9.5E-07****	**0.000****	1
	STNetKDE	**1.8E-05****	1	**9.5E-07****	**4.2E-04****

FC Feature Count, * significant at $\alpha = 0.05$ level, ** significant at $\alpha = 0.025$ level, XE-0Y = X*10^{-Y}

parameters help set the duration of the elevated crime risk, and the last determines how far it goes, as suggested by the near-repeat crime pattern (Farrell & Pease, 2001). For the current study, smoothing coefficients were reported to be mostly around 0.1, which indicates a prolonged temporal extent for crime incidents. On the other hand, SSRS values seemed to extend the spatial extent of the models, as evidenced by the greater SBW values of around 0.3 compared to those of other models, around 0.1. This increased spatial dependence signifies continuous risk fields between the selected urban features extending beyond a single street segment. The human activity flow between these features may play a key role in the strengthened connections between the neighboring segments, which may, in turn, help capture spatial spillover effects in crime risk (Wheeler, 2019). Lastly, the data-representation parameters have a far greater influence on the performance of the models than the learning rate. A possible reason is that this group of parameters adjusts the spatiotemporal extent of crime incidents. Since any crime prediction method heavily relies on these patterns, accurate data representation is of vital importance in terms of predictive performance.

The PCHM results demonstrated its effectiveness in enhancing hotspot predictions across both DL-based and baseline algorithms. Unlike previous research that achieved significant improvements by incorporating static POI data (Wang et al., 2016; Zhang et al., 2020) or ambient population figures (Malleson & Andresen, 2015; Hanaoka, 2018), the SSRS enhanced crime predictions with dynamic crime risk values. This improved performance supports the integration of a predominant boost perspective with a flag-based component that accounts for target attractiveness in the predictions (Pitcher & Johnson, 2011). While the former perspective can aptly describe individual offender behavior through an analogy to a 'forager,' the latter spatially contextualizes this forager by focusing on areas to which they are most attracted. In this sense, SSRS attempts to capture the attractiveness of street segments by monitoring intraday and weekly changes in crime risk around popular urban features. A secondary finding reveals that it is not merely the presence of risky urban features that drives environmental crime risk, but their actual exposure to crime. The reduced performance of models using feature counts largely supports this view. The vulnerability-exposure framework Kennedy et al. (2016) offers a fitting explanation for these dynamics. It suggests that the vulnerability posed by the presence of criminogenic buildings does not necessarily translate into higher crime rates in an area. This vulnerability must be actualized through exposure, which measures the crime prevalence in that environment based on past crime events. Our proposed SSRS aligns with this framework, as it quantifies the local effects of selected urban features on crime through the LRS, effectively integrating both vulnerability and exposure.

A key finding from our study demonstrates the superiority of graph learning algorithms (i.e., GraphWavenet, STCGN) over traditional DL algorithms like LSTM, and the selected baselines, MLP and STNetKDE in predicting crime hotspots across street networks. There are two primary factors responsible for this performance disparity. First, graph learning algorithms effectively capture spatial dependence through convolutional units that integrate information from neighboring segments. Research has consistently shown that crime risk emanates from the location of an initial crime event and spreads to nearby areas (Weisburd et al., 2006; Short et al., 2010). How this diffusion is modeled significantly influences the accuracy of crime prediction models

(Adepeju et al., 2016). Offenders often operate based on a mental template, which includes an opportunity map highlighting areas with high crime potential, known as awareness space (Brantingham & Brantingham, 1995). One limitation of traditional algorithms is their inability to model the described spatial diffusion effect. This may explain their lower accuracy in predicting across larger coverage areas (Figs. 11a and b and 12a and b), which likely encompass multiple segments. As a result, accounting for spatial diffusion significantly enhances the predictive power of graph-based models in this study. Secondly, the handling of temporal dependency differs between graph learning algorithms and traditional models. Graph models use convolutional units to manage temporal information, whereas LSTM relies on recurrent units, and MLP treats the sequences as input vectors. Recurrent units often lead to prolonged training times and issues with vanishing or exploding gradients as the length of the time series increases (Shleifer et al., 2019). On the other hand, MLP doesn't store information from past observations and is only able to capture temporal dependencies within the current time window. Given that crime prediction often requires long time series to capture patterns in sparse data Zhang and Cheng (2020), these algorithms may struggle with gradient problems, impacting their ability to capture these regularities effectively. This is reflected in the reduced MHR values for LSTM across various scenarios. On the other hand, graph learning algorithms employ fully convolutional units, making them more computationally efficient and quicker at training. Thus, using graph learning algorithms with convolutional units for modeling temporal dependencies presents a more effective alternative for enhancing the performance of Predictive Crime Hotspot Mapping (PCHM). One important point is that the consistent superiority of the graph learning algorithms over the non-neural network kernel-based baseline: STNetKDE. This superiority can justify the usage of more computationally expensive graph learning algorithms over a straightforward and more transparent counterpart.

Lastly, a noteworthy finding is the exceptional performance of MLP with SRSS in theft shift predictions, achieving an MHR of nearly 80%. This may be attributed to the distinct diurnal pattern of theft incidents across popular segments, regardless of their spatial dependence. Further analysis reveals that the crime concentration measure for the Central Side (CS) is 4.92%, which means 50% of theft incidents occur in 4.92% of the street segments. This indicates a high concentration of theft incidents within a smaller number of street segments. Coupled with the observation that yearly theft events in this area are significantly above the city average, it suggests that theft incidents are likely to concentrate in fewer street segments, facilitating more accurate crime prediction in this area.

Conclusion

In this study, we devised a novel network-based crime risk score, SSRS, that quantifies the dynamic crime risk of street segments based on the aggregated spatial influences of the hosted urban features. Next, we developed an auxiliary risk surface out of this score and incorporated it into intraday and daily PCHM models employing two graph learning algorithms (GWNet and STGCN), one traditional deep learning

algorithm(LSTM), and two baselines (MLP and STNetKDE). The effectiveness of the proposed risk surface manifested itself in the significant performance improvements across nearly all the models. Another important result indicated that the graph learning algorithms outperformed the traditional counterparts by a large margin due to their superior ability to capture spatiotemporal crime risk regularities. Lastly, the parameters related to data representation were found to have a significant impact on the performance of the selected algorithms, underlining the importance of properly introducing data to the crime prediction algorithms.

This study presents several research implications. Firstly, the significant performance improvements achieved by incorporating SSRS underscore the importance of contextualizing crime within its environmental setting. This context should encompass both boost and flag accounts of crime risk, which together can more accurately capture the dynamic interactions between offenders and their environment. Secondly, the variation in parameters across the models highlights the critical role of data representation. A key takeaway is that more precise data representation leads to more accurate predictions of crime hotspots. A data-driven approach, rather than a purely theoretical one, may thus be more effective for PCHM methods. Thirdly, the fact that graph learning algorithms doubled or even tripled the predictive performance of traditional LSTM, MLP, and STNetKDE demonstrates the importance of capturing spatial dependencies between neighboring units. Since crime occurs within a context, ignoring the interconnections between neighboring areas may undermine the effectiveness of predictions. Fourthly, convolutional units have proven more adept at capturing temporal dependencies in long, sparse time series. Crime time series, characterized by their sparsity due to the rarity of events, require modeling over extended sequential time steps. The challenges of vanishing or exploding gradients are significant drawbacks of LSTM, whose recurrent units may struggle as the size of time windows increases. Similarly, the inability of MLPs to capture spatiotemporal dependencies between events, particularly for rarer crimes like robbery, makes them prone to suboptimal predictive performance. However, MLP's impressive performance in shift theft predictions serves as a reminder of the varying role of spatiotemporal dependence across different crime events and contexts, particularly where crime is highly concentrated within a few segments. Lastly, employing complex and computationally intensive graph learning algorithms resulted in substantial improvements, achieving MHR levels significantly higher than those of STNetKDE—a traditional PCHM method that relies on spatiotemporal bandwidths fitted around crime incidents. This demonstrated superiority highlights the value of adopting sophisticated graph learning approaches for PCHM tasks.

This research also has several practical implications. First and foremost, Operationally, we treat SSRS as an environmental baseline—a stable, feature-driven indicator of a segment's underlying exposure—while the predicted crime risk is a transient outcome informed by the interaction of SSRS with recent incidents and temporal context (e.g., shift/time of day). This yields a simple, actionable rule for resource-constrained agencies: prioritize high-SSRS segments and modulate deployment using up-to-date crime history. In practice, late-night patrols emphasize high-SSRS segments proximate to pubs and groceries when recent incidents are present, whereas daytime patrols pivot to high-SSRS segments near fast-food outlets and bus

stops when recent activity signals elevated short-term risk. Second, the proposed approach helps create crime-specific maps, therefore they enact situational crime prevention that emphasizes the reduction of crime-specific risks by adopting suitable strategies (Clarke, 1995). In this case, while controlling access (i.e., gated entrance or exits) may be a suitable strategy for theft across the segments with higher predicted risk, increasing guardianship through the enhanced police presence may similarly reduce the robbery risk across the ones with higher predicted risk. The more targeted interventions also help save a significant amount of limited resources (e.g., time, police force, fuel) by optimizing patrol routes. Third, a training program can help place managers recognize the dynamic crime risks surrounding their places during a day or week. Informing them about the risky situations and how to enhance the security measures to reduce similar situations can further increase the safety across the streets (Eck et al., 2007). Lastly, one advantage of using this score is that it is bias-free, meaning that it doesn't involve any biased structural characteristics (e.g., Median Household Income, rate of unemployment, black population) whose incorporation often results in unfair risk calculations for the disadvantaged neighborhoods (Heaven, 2020). However, place-based scoring through can still stigmatize areas if high-SSRS segments are portrayed as inherently dangerous or repeatedly targeted. To use SSRS responsibly, practitioners should emphasize transparent communication: present scores as relative, provisional estimates rather than fixed labels; report uncertainty (e.g., confidence bands or stability ranges) and time-decay so users see that risk attenuates without recent incidents; and disclose data provenance.

The study presents several limitations. Firstly, our model is implemented only on the Center Side of Chicago due to the high computational complexity associated with the selected algorithms, particularly Graph WaveNet, for a citywide implementation. This model is prone to exponentially growing computational overheads in larger graphs (e.g., city graph) due to its adaptive dependency matrix. For example, the size of the current adaptive adjacency matrix is 6,046,081 (2459 nodes * 2459 nodes). Additionally, the total parameter count is 944,256, calculated as 8 (input channels) × 8 (output channels) × 2 (Kernel size) ×2459 (nodes) × 3 (layers). For a larger study area with 5000 street segments, the adjacency matrix would increase to 25,000,000, and the total parameter number would reach 1,920,000. The lack of scalability could seriously limit the generalizability of this study to larger areas. Secondly, DRSFs are highly sensitive to the spatial and temporal precision of reported crimes. Mislocated crime incidents or misreported times can severely distort the distance calculations and temporal distribution of crime, resulting in inaccurate modeling of spatial influences by the DRSFs. Thirdly, we selected only a limited set of urban features reported to have a significant spatial influence on crime, leaving the potential contributions of other influential urban features (e.g., subways, schools) unexplored. Finally, the computational complexities of Network K analysis and graph learning algorithms have impeded analysis at finer temporal granularity. For instance, the current study includes 731 daily and 2192 shift observations. Increasing the number of observations for hourly predictions would escalate to 14,620, posing a significant challenge for the proposed PCHM algorithms. Additionally, increasing the temporal granularity necessitates a corresponding increase in the number of models (space x time x crime) for Network K analysis, further compounding the challenge.

Future research holds promising directions for the current study. The first step forward should be to validate the proposed SSRS across different urban contexts. Given the unique characteristics of each setting, collaborating with security experts to develop context-specific SSRS models would represent an important contribution. A potential direction may be to implement our models with finer temporal granularities. For instance, an algorithm that tracks two-hourly or six-hourly crime risk changes may further improve crime hotspot predictions. Another direction is to examine the applicability of different techniques in calculating DRSFs. For example, nonlinear functions may better capture the dynamic and curvilinear spatial influence around the urban features. A valuable next step is to calculate SSRSs for violent crimes (e.g., assault, homicide), which tend to show more irregular patterns (Mohler et al.,2011). Another interesting direction would be to test the effectiveness of the developed PCHM during and after COVID, which has been shown to have a significant impact on crime patterns (Campedelli et al., 2020). Future researchers may wish to implement the latest spatiotemporal graph learning algorithms (e.g., Ma et al., 2023) and compare their performances with those in the current study for PCHM tasks. Lastly, applying a hierarchical approach to examine how the proposed SSRS interacts with the social context (e.g., the demographic structure of the study area) would provide valuable insights into the processes underlying crime patterns.

Acknowledgements The authors would like to thank Dr. James Ward for his outstanding contribution to the proofreading of the current manuscript.

Authors' Contributions Tugrul Cabir Hakyemez: Conceptualization, Methodology, Data curation, Formal Analysis, Writing- Original draft preparation, Visualization, Investigation, Writing - Review & Editing. Bertan Badur: Conceptualization, Methodology, Supervision.

Funding Open access funding provided by the Scientific and Technological Research Council of Türkiye (TÜBİTAK). This research was funded by Bogazici University Scientific Research Fund, grant number 15385D.

Data Availability The datasets and detailed results are available with a DOI: https://doi.org/10.6084/m9.figshare.25106126 in the link:
https://figshare.com/s/a81644981243dfe301df.

Declarations

Conflict of interest The authors declare no conflict of interest.

Open Access This article is licensed under a Creative Commons Attribution 4.0 International License, which permits use, sharing, adaptation, distribution and reproduction in any medium or format, as long as you give appropriate credit to the original author(s) and the source, provide a link to the Creative Commons licence, and indicate if changes were made. The images or other third party material in this article are included in the article's Creative Commons licence, unless indicated otherwise in a credit line to the material. If material is not included in the article's Creative Commons licence and your intended use is not permitted by statutory regulation or exceeds the permitted use, you will need to obtain permission directly from the copyright holder. To view a copy of this licence, visit http://creativecommons.org/licenses/by/4.0/.

References

Adepeju, M., Rosser, G., & Cheng, T. (2016). Novel evaluation metrics for sparse spatio-temporal point process hotspot predictions-a crime case study. *International Journal of Geographical Information Science*, *30*(11), 2133–2154. https://doi.org/10.1080/13658816.2016.1159684

Al-Sabbagh, T. A., Li, Y., Lee, Y. J., & El Kenawy, A. M. (2024). Land use and sexual harassment: A geo-spatial analysis based on the volunteer HarassMap-Egypt. *Geographical Research, 62*(1), 147–164. https://doi.org/10.1111/1745-5871.12619

Ariel, B., & Partridge, H. (2017). Predictable policing: Measuring the crime control benefits of hotspots policing at bus stops. *Journal of Quantitative Criminology*, *33*(4), 809–833.

Baddeley, A. (2005). R. (Ed.), Spatstat: An R package for Analyzing Spatial point patterns. *Journal of Statistical Software* 12 https://doi.org/10.18637/jss.v012.i06.

Baddeley, A., Diggle, P. J., Hardegen, A., Lawrence, T., Milne, R. K., & Nair, G. (2014). On tests of spatial pattern based on simulation envelopes. *Ecological Monographs, 84*(3), 477–489. https://doi.org/10.1890/13-2042.1

Barnum, J. D., Caplan, J. M., Kennedy, L. W., & Piza, E. L. (2017). The crime kaleidoscope: A cross-jurisdictional analysis of place features and crime in three urban environments. *Applied Geography, 79*, 203–211. https://doi.org/10.1016/j.apgeog.2016.12.011

Bengio, Y. (2012). Practical recommendations for gradient-based training of deep architectures. G. B. Orr in, *Neural networks: Tricks of the trad* (Volume 7700, s. 437–478). Berlin: Springer.

Bernasco, W. (2010). Modeling micro-level crime location choice: Application of the discrete choice framework to crime at places. *Journal of Quantitative Criminology*, *26*(1), 113–138. https://doi.org/10.1007/s10940-009-9086-6

Bernasco, W., & Block, R. (2009). Where offenders choose to attack: A discrete choice model of robberies in Chicago. *Criminology*, *47*(1), 93–130. https://doi.org/10.1111/j.1745-9125.2009.00140.x

Bernasco, W., & Block, R. (2011). Robberies in chicago: A block-level analysis of the influence of crime generators, crime attractors, and offender anchor points. *Journal of Research in Crime and Delinquency*, *48*(1), 33–57. https://doi.org/10.1177/0022427810384135

Bernasco, W., & Nieuwbeerta, P. (2005). How do residential burglars select target areas? A new approach to the analysis of criminal location choice. *British Journal of Criminology*, *45*(3), 296–315. https://doi.org/10.1093/bjc/azh070

Bernasco, W., Ruiter, S., & Block, R. (2017). Do street robbery location choices vary over time of day or day of week? A test in Chicago. *Journal of Research in Crime and Delinquency, 54*(2), 244–275. https://doi.org/10.1177/0022427816680681

Block, R. L., & Block, C. R. (1995). Space, place and crime: Hot spot areas and hot places of liquor-related crime. *Crime and Place, 4*(2), 145–184.

Bowers, K. J., Johnson, S. D., & Pease, K. (2004). Prospective hot-spotting: The future of crime mapping? *British Journal of Criminology, 44*(5), 641–658. https://doi.org/10.1093/bjc/azh036

Brantingham, P., & Brantingham, P. (1981). *Environmental Criminology*. Sage Publications.

Brantingham, P., & Brantingham, P. (1995). Criminality of place. *European Journal on Criminal Policy and Research*, *3*, 5–26. https://doi.org/10.1007/BF02242925

Bronstein, M. M., Bruna, J., Cohen, T., & Veličković, P. (2021). Geometric deep learning: Grids, groups, graphs, geodesics, and gauges. *ArXiv Preprint*, 210413478. https://doi.org/10.48550/arXiv.2104.13478

Campedelli, G. M., Favarin, S., Aziani, A., & Piquero, A. R. (2020). Disentangling community-level changes in crime trends during the COVID-19 pandemic in Chicago. *Crime Science, 9*, 1–18. https://doi.org/10.1186/s40163-020-00131-8

Caplan, J. M., Kennedy, L. W., & Miller, J. (2011). Risk terrain modeling: Brokering criminological theory and GIS methods for crime forecasting. *Justice Quarterly, 28*(2), 360–381. https://doi.org/10.1080/07418825.2010.486037

Cheng, T., & Adepeju, M. (2014). Modifiable temporal unit problem (MTUP) and its effect on space-time cluster detection. *PLoS One,* (5), Article e100465. https://doi.org/10.1371/journal.pone.0100465

Chicago Police Department (2021). *PAYROLL AND TIMEKEEPING - ATTENDANCE.* URL: http://directives.chicagopolice.org/directives/data/a7a57b36-12cf4df7-24112-cf4e-9398046d4f55fbaf.html Accessed on: September 19, 2021.

Clarke, R. V. (1995). Situational crime prevention. *Crime and Justice, 19*, 91–150. https://doi.org/10.1086/449230

Cohen, L. E., & Felson, M. (1979). Social change and crime rate trends: A routine activity approach. *American Sociological Review, 44*(4), 588–608. https://doi.org/10.2307/2094589

Corcoran, J. J., Wilson, I. D., & Ware, J. A. (2003). Predicting the geo-temporal variations of crime and disorder. *International Journal of Forecasting, 19*(4), 623–634. https://doi.org/10.1016/S0169-2070(03)00095-5

Cornish, D. B., & Clarke, R. V. (1987). Understanding crime displacement: An application of rational choice theory. *Criminology, 25*(4), 933–948. https://doi.org/10.1111/j.1745-9125.1987.tb00826.x

D Heaven, W. (2020). Predictive policing algorithms are racist. They need to be dismantled. *MIT Technology Review*, *17*, 2020.

Defferrard, M., Bresson, X., & Vandergheynst, P. (2016). Convolutional neural networks on graphs with fast localized spectral filtering. *Advances in neural information processing systems* (s. 3844–3852). Barcelona: NIPS.

Drawve, G. (2016). A metric comparison of predictive hot spot techniques and RTM. *Justice Quarterly*, *33*(3), 363–397. https://doi.org/10.1080/07418825.2014.904393

Drawve, G., Thomas, S. A., & Walker, J. T. (2016). Bringing the physical environment back into neighborhood research: The utility of RTM for developing an aggregate neighborhood risk of crime measure. *Journal of Criminal Justice, 44*, 21–29. https://doi.org/10.1016/j.jcrimjus.2015.12.002

Eck, J. E., Clarke, R. V., & Guerette, R. T. (2007). Risky facilities: Crime concentration in homogeneous sets of establishments and facilities. *Crime Prevention Studies, 21*, 225.

Farrell, G., & Pease, K. (2001). *Repeat victimization*. Criminal Justice.

Goodfellow, I., Bengio, Y., & Courville, A. (2016). *Deep learning*. MIT Press.

Groff, E. (2011). Exploring 'near': Characterizing the spatial extent of drinking place influence on crime. *Australian & New Zealand Journal of Criminology, 44*(2), 156–179. https://doi.org/10.1177/0004865811405253

Groff, E. (2017). Measuring the influence of the built environment on crime at street segments. *Jerusalem Review of Legal Studies*, *15*(1), 44–54. https://doi.org/10.1093/jrls/jlx005

Groff, E. R., & La Vigne, N. G. (2002). Forecasting the future of predictive crime mapping. *Crime Prevention Studies, 12*, 29–58.

Groff, E., & Lockwood, B. (2014). Criminogenic facilities and crime across street segments in Philadelphia: Uncovering evidence about the Spatial extent of facility influence. *Journal of Research in Crime and Delinquency, 51*(3), 277–314. https://doi.org/10.1177/0022427813512494

Grubesic, T. H., & Mack, E. A. (2008). Spatio-temporal interaction of urban crime. *Journal of Quantitative Criminology, 24*(3), 285–306. https://doi.org/10.1007/s10940-008-9047-5

Gu, H., Sui, J., & Chen, P. (2024). Graph representation learning for street-Level Crime Prediction. *ISPRS International Journal of Geo-Information, 13*(7), Article 229. https://doi.org/10.3390/ijgi13070229

Haberman, C. P., & Ratcliffe, J. H. (2015). Testing for temporally differentiated relationships among potentially criminogenic places and census block street robbery counts. *Criminology, 53*(3), 457–483. https://doi.org/10.1111/1745-9125.12076

Hakyemez, T. C., & Badur, B. (2021). Crime risk stations: Examining Spatiotemporal Influence of Urban Features through Distance-Aware Risk Signal Functions. *ISPRS International Journal of Geo-Information, 10*(7), Article 472. https://doi.org/10.3390/ijgi10070472

Hakyemez, T. C., & Badur, B. (2023). Incorporating park events into crime hotspot prediction on street networks: A spatiotemporal graph learning approach. *Applied Soft Computing, 148*, Article 110886. https://doi.org/10.1016/j.asoc.2023.110886

Hanaoka, K. (2018). New insights on relationships between street crimes and ambient population: Use of hourly population data estimated from mobile phone users' locations. *Environment and Planning B: Urban Analytics and City Science*, *45*(2), 295–311. https://doi.org/10.1177/0265813516672454

Hart, T. C., & Miethe, T. D. (2015). Configural behavior settings of crime event locations: Toward an alternative conceptualization of criminogenic microenvironments. *Journal of Research in Crime and Delinquency, 52*(3), 373–402. https://doi.org/10.1177/0022427814566639

Hipp, J. R., Lee, S., Ki, D., & Kim, J. H. (2021). Measuring the built environment with Google Street View and machine learning: Consequences for crime on street segments. *Journal of Quantitative Criminology*. https://doi.org/10.1007/s10940-021-09506-9

Hou, M., Hu, X., Cai, J., Han, X., & Yuan, S. (2022). An integrated graph model for spatial–temporal urban crime prediction based on attention mechanism. *ISPRS International Journal of Geo-Information, 11*(5), Article 294. https://doi.org/10.3390/ijgi11050294

Huang, C., Zhang, J., Zheng, Y., & Chawla, N. V. (2018). DeepCrime: Attentive hierarchical recurrent networks for crime prediction. *Proceedings of the 27th ACM International Conference on Information and Knowledge Management* (s. 1423–1432). Torino: ACM.

Irvin-Erickson, Y., & La Vigne, N. (2015). A spatio-temporal analysis of crime at Washington, DC metro rail: Stations' crime-generating and crime-attracting characteristics as transportation nodes and places. *Crime Science, 4*, 1–13. https://doi.org/10.1186/s40163-015-0026-5

Jin, G. L., Sha, C. X. Z., Liu, H., Y., & Huang, J. (2022). Adaptive dual-view Wavenet for urban spatial–Temporal event prediction. *Information Sciences*, *588*, 315–330. https://doi.org/10.1016/j.ins.2021.12.085

Jin, G., Sha, H., Xi, Z., & Huang, J. (2023). Urban hotspot forecasting via automated spatio-temporal information fusion. *Applied Soft Computing, 136*, Article 110087. https://doi.org/10.1016/j.asoc.2023.110087

Johnson, S. D., & Bowers, K. J. (2004). The burglary as clue to the future: The beginnings of prospective hot-spotting. *European Journal of Criminology, 1*(2), 237–255. https://doi.org/10.1177/1477370804041252

Johnson, S. D., Summers, L., & Pease, K. (2009). Offender as forager? A direct test of the boost account of victimization. *Journal of Quantitative Criminology, 25*(2), 181–200.

Kadar, C., Maculan, R., & Feuerriegel, S. (2019). Public decision support for low population density areas: An imbalance-aware hyper-ensemble for spatio-temporal crime prediction. *Decision Support Systems*, *119*, 107–117. https://doi.org/10.1016/j.dss.2019.03.001

Kennedy, L. W., Caplan, J. M., Piza, E. L., & Buccine-Schraeder, H. (2016). Vulnerability and exposure to crime: Applying risk terrain modeling to the study of assault in Chicago. *Applied Spatial Analysis and Policy, 9*(4), 529–548. https://doi.org/10.1007/s12061-015-9165-z

Kim, H. J., Fay, M. P., Feuer, E. J., & Midthune, D. N. (2000). Permutation tests for joinpoint regression with applications to cancer rates. *Statistics in Medicine, 19*(3), 335–351. https://doi.org/10.1002/(SICI)1097-0258(20000215)19:3<335::AID-SIM336>3.0.CO;2-Z

Krizhevsky, A., Sutskever, I., & Hinton, G. E. (2012). Imagenet classification with deep convolutional neural networks. *Advances in neural information processing systems* (s. 1097–1105). Stateline,NV: NeurIPS. https://proceedings.neurips.cc/paper/2012/file/c399862d3b9d6b76c8436e924a68c45b-Paper.pdf

Ma, M., Xie, P., Teng, F., Wang, B., Ji, S., Zhang, J., & Li, T. (2023). HiSTGNN: Hierarchical spatio-temporal graph neural network for weather forecasting. *Information Sciences, 648*, Article 119580. https://doi.org/10.1016/j.ins.2023.119580

Malleson, N., & Andresen, M. A. (2015). Spatio-temporal crime hotspots and the ambient population. *Crime Science*, *4*, 1–8. https://doi.org/10.1186/s40163-015-0023-8

Mohler, G. O., Short, M. B., Brantingham, P. J., Schoenberg, F. P., & Tita, G. E. (2011). Self-exciting point process modeling of crime. *Journal of the American Statistical Association, 106*(493), 100–108. https://doi.org/10.1198/jasa.2011.ap09546

Ohyama, T., & Amemiya, M. (2018). Applying crime prediction techniques to Japan: A comparison between risk terrain modeling and other methods. *European Journal on Criminal Policy & Research, 24*(4), 469–487.

Okabe, A., & Sugihara, K. (2012). *Spatial analysis along networks: Statistical and computational methods.* John Wiley & Sons.

Okabe, A., Satoh, T., & Sugihara, K. (2009). A kernel density estimation method for networks, its computational method and a GIS-based tool. *International Journal of Geographical Information Science, 23*(1), 7–32. https://doi.org/10.1080/13658810802475491

Olligschlaeger, A. M. (1997). Artificial neural networks and crime mapping. *Crime mapping and crime prevention, 1*, 313.

Pease, K. (1998). *Repeat victimisation: Taking stock.* Home Office Police Research Group.

Pitcher, A. B., & Johnson, S. D. (2011). Exploring theories of victimization using a mathematical model of burglary. *Journal of Research in Crime and Delinquency, 48*(1), 83–109. https://doi.org/10.1177/0022427810384139

Pred, A. (1981). Social reproduction and the time-geography of everyday life. *Geografiska Annaler. Series B, Human Geography, 63*(1), 5–22. https://doi.org/10.2307/490994

Ratcliffe, J. H. (2006). A temporal constraint theory to explain opportunity-based spatial offending patterns. *Journal of Research in Crime and Delinquency, 43*(3), 261–291. https://doi.org/10.1177/0022427806286566

Ratcliffe, J. H. (2012). The spatial extent of criminogenic places: A changepoint regression of violence around bars. *Geographical Analysis, 44*(4), 302–320. https://doi.org/10.1111/j.1538-4632.2012.00856.x

Repetto, T. A. (1976). Crime prevention and the displacement phenomenon. *Crime*.

Rosser, G., & Cheng, T. (2019). Improving the robustness and accuracy of crime prediction with the self-exciting point process through isotropic triggering. *Applied Spatial Analysis and Policy*, *12*(1), 5–25. https://doi.org/10.1007/s12061-016-9198-y

Rosser, G., Davies, T., Bowers, K. J., Johnson, S. D., & Cheng, T. (2017). Predictive crime mapping: Arbitrary grids or street networks? *Journal of Quantitative Criminology*, *33*(3), 569–594. https://doi.org/10.1007/s10940-016-9321-x

Rummens, A., Hardyns, W., & Pauwels, L. (2017). The use of predictive analysis in spatiotemporal crime forecasting: Building and testing a model in an urban context. *Applied Geography, 86*, 255–261. https://doi.org/10.1016/j.apgeog.2017.06.011

Safat, W., Asghar, S., & Gillani, S. A. (2021). Empirical analysis for crime prediction and forecasting using machine learning and deep learning techniques. *Ieee Access : Practical Innovations, Open Solutions*, *9*, 70080–70094. https://doi.org/10.1109/ACCESS.2021.3078117

Sherman, L. W., & Weisburd, D. (1995). General deterrent effects of police patrol in crime "hot spots": A randomized, controlled trial. *Justice Quarterly, 12*(4), 625–648. https://doi.org/10.1080/07418829500096221

Sherman, L. W., Gartin, P. R., & Buerger, M. E. (1989). Hot spots of predatory crime: Routine activities and the criminology of place. *Criminology, 27*(1), 27–56. https://doi.org/10.1111/j.1745-9125.1989.tb00862.x

Shleifer, S., McCreery, C., & Chitters, V. (2019). Incrementally improving graph Wavenet performance on traffic prediction. *ArXiv Preprint*, *912.07390*. arXiv:1912.07390v1

Short, M. B., Brantingham, P. J., Bertozzi, A. L., & Tita, G. E. (2010). Dissipation and displacement of hotspots in reaction-diffusion models of crime. *Proceedings of the National Academy of Sciences, 107*(9), 3961–3965. https://doi.org/10.1073/pnas.0910921107

Smith, M. (2018, October 30). *Can we predict when and where a crime will take place?* BBC: URL: https://www.bbc.com/news/business-46017239 Last accessed on May 1, 2024.

Summers, L., & Caballero, M. (2017). Spatial conjunctive analysis of (crime) case configurations: Using Monte Carlo methods for significance testing. *Applied Geography*, *84*, 55–63. https://doi.org/10.1016/j.apgeog.2017.05.002

Van Den Oord, A., Dieleman, S., Zen, H., Simonyan, K., Vinyals, O., Graves, A., & Kavukcuoglu, K. (2016). WaveNet: A generative model for Raw audio. *SSW*, *125*(2).

Vandeviver, C., Neirynck, E., & Bernasco, W. (2023). The foraging perspective in criminology: A review of research literature. *European Journal of Criminology*, *20*(2), 626–652. https://doi.org/10.21428/cb6ab371.a832e977

Wang, J. (2017, December). *This Is a Story About Nerds and Cops: PredPol and Algorithmic Policing*. URL: https://www.e-flux.com/journal/87/169043/this-is-a-story-about-nerds-and-cops-predpol-and-algorithmic-policing/

Wang, H., Kifer, D., Graif, C., & Li, Z. (2016). Crime rate inference with big data. *Proceedings of the 22nd ACM SIGKDD international conference on knowledge discovery and data mining* (s. 635–644). San Francisco, CA: ACM. https://doi.org/10.1145/2939672.2939736

Wang, C., Lin, Z., Yang, X., Sun, J., Yue, M., & Shahabi, C. (2022). Homophily-aware graph convolutional recurrent network for crime forecasting. Proceedings of the AAAI Conference on Artificial Intelligence (pp. 4193–4200). Hagen: AAAI.

Weisburd, D. (2015). The law of crime concentration and the criminology of place. *Criminology*, *53*(2), 133–157. https://doi.org/10.1111/1745-9125.12070

Weisburd, D., Wyckoff, L. A., Ready, J., Eck, J. E., Hinkle, J. C., & Gajewski, F. (2006). Does crime just move around the corner? A controlled study of Spatial displacement and diffusion of crime control benefits. *Criminology*, *44*(3), 549–592. https://doi.org/10.1111/j.1745-9125.2006.00057.x

Weisburd, D., Groff, E. R., & Yang, S. M. (2012). *The criminology of place: Street segments and our understanding of the crime problem.* Oxford University Press.

Wheeler, A. P. (2019). Quantifying the local and spatial effects of alcohol outlets on crime. *Crime & Delinquency, 65*(6), 845–871. https://doi.org/10.1177/0011128718806692

Wu, Z., Pan, S., Long, G., Jiang, J., & Zhang, C. (2019). Graph Wavenet for deep spatial-temporal graph modeling. *ArXiv Preprint*, 1906.00121. doi:arXiv:1906.00121.

Yu, B., Yin, H., & Zhu, Z. (2018). Spatio-temporal graph convolutional networks: A deep learning framework for traffic forecasting. *IJCAI*, (s. 3634–3640). Stockholm.

Yue, H., Zhu, X., Ye, X., & Guo, W. (2017). The local colocation patterns of crime and land-use features in Wuhan, China. *ISPRS International Journal of Geo-Information, 6*(10), Article 307. https://doi.org/10.3390/ijgi6100307

Zhang, Y., & Cheng, T. (2020). Graph deep learning model for network-based predictive hotspot mapping of sparse spatio-temporal events. *Computers, Environment and Urban Systems, 79*, Article 101403. https://doi.org/10.1016/j.compenvurbsys.2019.101403

Zhang, X., Liu, L., Xiao, L., & Ji, J. (2020). Comparison of machine learning algorithms for predicting crime hotspots. *Ieee Access : Practical Innovations, Open Solutions*, *8*, 181302–181310. https://doi.org/10.1109/ACCESS.2020.3028420

Zhuang, Y., Almeida, M., Morabito, M., & Ding, W. (2017). Crime hot spot forecasting: A recurrent model with spatial and temporal information. *IEEE International Conference on Big Knowledge (ICBK)* (s. 143–150). Hefei: IEEE. https://doi.org/10.1109/ICBK.2017.3

Publisher's Note Springer Nature remains neutral with regard to jurisdictional claims in published maps and institutional affiliations.